Molecular Pharmacology Fast Forward. Published on September 27, 2007 as doi:10.1124/mol.107.036285

MOL #36285

Alternative translation initiation of human RGS2 yields a set of functionally distinct proteins.

Steven Gu, Annepa Anton, Samina Salim , Kendall J. Blumer, Carmen W. Dessauer, and Scott P. Heximer

Department of Physiology, Heart and Stroke/Richard Lewar Centre of Excellence in Cardiovascular Research (S.G., A.A., S.P.H.) University of Toronto, 1 King's College Circle, Toronto, Ontario M5S 1A8. Department of Integrative Biology and Pharmacology, University of Texas Health Science Center at Houston, 6431 Fannin St., Houston, Texas 77030 (S.S., C.W.D.) Department of Cell Biology and Physiology, Washington University School of Medicine, 660 South Euclid Avenue, St. Louis, Missouri 63110 (K.J.B.)

To whom all correspondence should be addressed:

scott.heximer@utoronto.ca
Phone (416) 978-6048
Fax (416) 978-4373

Molecular Pharmacology Fast Forward. Published on September 27, 2007 as DOI: 10.1124/mol.107.036285
This article has not been copyedited and formatted. The final version may differ from this version.

Running Title: Translation-level regulation of RGS2 function

Corresponding author:

Scott P. Heximer
Canada Research Chair in Cardiovascular Physiology
scott.heximer@utoronto.ca
Phone (416) 978-6048
Fax (416) 978-4940

Word Count:

Abstract: 241
Introduction: 406
Discussion: 1224

Pages: 41
Tables: 1
Figures: 8
References: 40

List of Abbreviations: G-protein; guanine nucleotide binding protein, 7TMR; 7 transmembrane receptor, GTP; guanosine triphosphate, cAMP; cyclic adenosine monophosphate, RGS, regulator of G-protein signaling, AC, adenylyl cyclase; ACV, type V adenylyl cyclase; NTD, amino terminal domain; NT, amino terminus; ORF, open reading frame; GAP; GTPase activating protein, GFP; green fluorescent protein, cDNA; complementary DNA, HRP, horseradish peroxidase, ROI; region of interest, IBMX; 3-isobutyl-1-methylxanthine, HBSS; HEPES buffered saline solution, RIA; radioimmunoassay, TMRM; tetramethyl rhodamine methyl ester

Molecular Pharmacology Fast Forward. Published on September 27, 2007 as DOI: 10.1124/mol.107.036285
This article has not been copyedited and formatted. The final version may differ from this version.

ABSTRACT

The regulator of G-protein signaling RGS2 contains a characteristic RGS domain flanked by short amino and carboxyl terminal sequences. The RGS domain mediates inhibition of $G\alpha_q$ and $G\alpha_i$ signaling, while the amino terminal domain (NTD) directs interaction with adenylyl cyclases, GPCRs and other signaling partners. Here, we identify a set of novel RGS2 protein products that differ with respect to their amino terminal architecture and functional characteristics. An RGS2 expression reporter cassette revealed four distinct open reading frames that can be expressed from the RGS2 NTD. We hypothesized that alternative translation initiation from four AUG codons corresponding to amino acid positions 1, 5, 16, and 33 could produce the observed RGS2 expression profile. Selective disruption of each AUG confirmed that alternate sites of translation initiation accounted for each of the observed products. Proteins derived from ORFs 1-4 showed no difference in $G\alpha_q$ inhibitory potential or recruitment from the nucleus in response to $G\alpha_q$ signaling. By contrast, RGS2 products initiating from methionines at positions 16 (ORF3) and 33 (ORF4) were impaired as inhibitors of type V adenylyl cyclase (ACV) compared to full length RGS2. We predicted that regulation of the RGS2 expression profile would allow cells to adapt to changing signaling conditions. Consistent with this model, activation of $G\alpha_s$/ ACV but not $G\alpha_q$ signaling increased the relative abundance of the full-length RGS2 protein suggesting that alternative translation initiation of RGS2 is part of a novel negative feedback control pathway for adenylyl cyclase signaling.

Molecular Pharmacology Fast Forward. Published on September 27, 2007 as DOI: 10.1124/mol.107.036285
This article has not been copyedited and formatted. The final version may differ from this version.

INTRODUCTION

Heterotrimeric G-protein coupled receptors mediate cell responses to a variety of extracellular ligands (Ma and Zemmel, 2002). Coordination of G-protein signaling allows cells to adjust rapidly to dynamic physiologic conditions. Mammalian *r*egulators of *G*-protein *s*ignaling (RGS) proteins attenuate G-protein α subunit activity via GTPase activating protein (GAP) domains (Berman *et al.*, 1996; Watson *et al.*, 1996) and thus are important for signal modulation and discrimination. A number of RGS proteins contain activities that extend beyond their GAP function. Proteins within the RGS7-like, RGS12-like, RhoGEF-containing, and G protein-coupled receptor kinase-like RGS protein subfamilies contain multiple modular protein-protein interaction domains that allow them to coordinate signaling between intracellular signaling networks (Ross and Wilkie, 2000; Zheng *et al.*, 1999). By comparison, simply constructed RGS proteins in the RGSZ-like and RGS4-like (R4/B) subfamilies consist of little more than an RGS domain flanked by short (typically 10 to 70 residues) amino- and carboxyl-terminal extensions. It is evident that even such simple RGS proteins can be versatile integrators of G-protein signaling through their interaction with a diverse number of intracellular protein partners (Heximer and Blumer, 2007).

RGS2 belongs to the R4/B subfamily of simple RGS proteins. Despite its small size RGS2 can interact with G-proteins and non-G-protein signaling partners. The GAP domain of RGS2 inhibits $G\alpha_q$- (Heximer *et al.*, 1999), and $G\alpha_i$- (Ingi *et al.*, 1998) signaling, while sequences within the RGS2 amino terminal domain (NTD) direct nuclear and plasma membrane targeting (Heximer *et al.*, 2001). More recently, however, the

Molecular Pharmacology Fast Forward. Published on September 27, 2007 as DOI: 10.1124/mol.107.036285
This article has not been copyedited and formatted. The final version may differ from this version.

NTD of RGS2 has also been shown to interact with additional signaling partners including GPCR third intracellular loops and spinophilin (Bernstein *et al.,* 2004; Hague *et al.*, 2005; Wang *et al.*, 2005), adenylyl cyclase (Roy *et al.*, 2006a; Salim *et al.*, 2003; Sinnarajah *et al.*, 2001) and TRPV6 (Schoeber *et al.*, 2006) and tubulin (Heo *et al.*, 2006). Importantly, engagement of the versatile RGS2 NTD with various signaling partners is expected to direct the carboxyl terminal GAP domain into context-specific signaling compartments.

Several RGS genes produce more than one protein with unique functional properties using alternative mRNA splicing. Chidiac and coworkers recently showed that multiple RGS2 bands were evident in forskolin stimulated mouse osteoblasts (Roy *et al.*, 2006b). We examined the possible mechanisms that might result in the production of multiple RGS2 proteins. A search of the human expressed sequence tag database (NLM/NCBI) revealed no evidence of alternatively spliced *RGS2* mRNAs. Furthermore, our own expression data suggested that multiple RGS2 proteins are expressed from the full *RGS2* cDNA alone (Heximer *et al.*, 1999). Together, these observations prompted us to study whether alternative translation of the human *RGS2* mRNA was important for the regulation of its expression and function. Here, we report the discovery of a novel set of alternatively translated RGS2 protein proteins with distinct functional properties whose relative expression levels are coupled to changes in cell signaling status.

Molecular Pharmacology Fast Forward. Published on September 27, 2007 as DOI: 10.1124/mol.107.036285
This article has not been copyedited and formatted. The final version may differ from this version.

MATERIALS AND METHODS

Materials-- The pEGFP-C1 or pREV-TRE (Clontech; Palo Alto, CA) plasmids were used to express RGS2 in this study. Constitutively active $G\alpha_q$(R183C) construct in pCIS was a kind gift from Dr. J. Hepler (Emory University, Atlanta, GA). Constitutively active $G\alpha_s$ (GsQ227L) and the ACV clone were kindly provided by Drs. R. Feldman and P. Chidiac (University of Western Ontario, London, ON). Expression constructs for Fibrillarin-HcRed were kindly donated by Dr. K. Lukyanov (Shemyakin and Ovchinnikov Institute of Bioorganic Chemistry, Moscow, Russia). Polyclonal anti-GFP antibody was from Clontech (cat# 632376) and HRP-coupled goat anti-rabbit IgG secondary and mouse 9E10 monoclonal anti-myc epitope antibodies were from Covance Research Products (Denver, PA). HEK293 cells stably expressing the M1 muscarinic receptor were kindly provided by P. Burgon and E. Peralta. Tet-ON HEK293 cells were from Clontech. All culture medium components were from Invitrogen (Burlington, ON). Myo-[^{3}H] inositol for cell labeling studies was from Amersham Biosciences (Baie D'Urfe, PQ). FuGENE 6 transfection reagent was purchased from Roche Diagnostics (Laval, PQ). The cyclic AMP enzyme immunoassay kits were from Biomedical Technologies Inc. (Stoughton, MA) and Assay Designs, Inc. (Ann Arbor, MI). Unless otherwise stated, all other reagents and chemicals were from Sigma (Oakville, ON).

cDNA Constructs—cDNA expression constructs were amplified by high fidelity polymerase chain reaction (*Pfu*, Stratagene, La Jolla, CA) and cloned into the *Nhe* I and *Age* I cloning sites ahead of enhanced green fluorescent protein (GFP) in pEGFP-C1. Where indicated, a Kozak consensus translation initiation sequence

Molecular Pharmacology Fast Forward. Published on September 27, 2007 as DOI: 10.1124/mol.107.036285
This article has not been copyedited and formatted. The final version may differ from this version.

(GCCACCATGGCG) was introduced to increase the efficiency of translation of the different potential initiator codons. The following 5' PCR primers were used to generate the various RGS2 amino terminal constructs used in this study: wild type full-length (no Kozak consensus), 5'-ACTAGTATGCAAAGTGCTATGTTC-3'; Kozak full-length (kzORF1), 5'-ACTAGTGGATCCGCCACCATGGCGCAAAGTGCTATGTTCTTG-3'; kzORF2, 5'-ACTAGTGGATCCGCCACCATGGCGTTCTTGGCTGTTCAACAC-3'; kzORF3, 5'-ACTAGTGGATCCGCCACCATGGCGGACAAGAGCGCAGGCAGT-3'; and kzORF4, 5'-ACTAGTGGATCCGCCACCATGGCGAAACGGACCCTTTTAAAAGATTGG-3'; in combination with a common 3' primer 5'- ACCGGTCGGTTCAAGTCTTCTTCTGA-3. To create the translation initiation reporter construct used to determine relative usage of initiator codon use in the *RGS2* mRNA, cDNA sequences spanning the complete 5' untranslated region (upstream primer, 5'-GCTAGCGCAAACAGCCGGGGCT-3') and coding sequence for amino acid residues 1-79 (downstream primer, 5'-ACCGGTCGCAGCTGTGCTTCCTCAGG-3' were cloned ahead of GFP as described above. RGS2 point mutations were made using the QuikChange mutagenesis kit (Stratagene). All constructs were purified using an Endo-Free Maxi^{TM} large scale DNA purification kit (Qiagen, Mississauga, ON) and verified by DNA sequencing of the entire protein-coding region.

Cell lines and Tissue Culture— HEK293 and Tet-ON HEK293 cells were maintained in Dulbecco's modified Eagle's medium (DMEM): Ham's F12 medium (1:1) and α-MEM

Molecular Pharmacology Fast Forward. Published on September 27, 2007 as DOI: 10.1124/mol.107.036285
This article has not been copyedited and formatted. The final version may differ from this version.

respectively, supplemented with 10% (v/v) heat-inactivated fetal calf serum (Atlanta Biologicals, Lawerenceville, GA), 2 mM glutamine, 10 µg/ml streptomycin, and 100 units/ml penicillin at 37 °C in a humidified atmosphere with 5% CO_2. For doxycycline induction studies, transiently transfected Tet-ON HEK293 cells were treated for 48 hrs with the indicated doxycycline concentrations before harvesting for immunoblotting. All stably transfected HEK293 cell lines expressing epitope-tagged RGS2 were generated essentially as described previously (Heximer *et al.*, 1999). Briefly, a clonal population HEK293 cells (7 x 10^6 cells in 10 cm plates) was transfected with 5 µg of mammalian expression constructs that direct expression of translation start-site optimized and wild type RGS2 constructs that had been tagged at their carboxyl-termini with three tandem copies of the c-myc epitope. Cells were plated at limiting dilution and stable RGS2-$(myc)_3$-expressing clones were selected for in growth medium containing 0.5mg/ml genetecin. Cell lines expressing similar levels of RGS2 protein were identified by Western blotting and clonality was verified by immunofluorescence staining using the mouse 9E10 monoclonal antibody. Clonal cell lines were immediately frozen in aliquots for storage at passage 3-4. The possibility of that loss of the appropriate signaling molecules occurred during clonal selection was minimized by examination of the relevant signaling readouts in 22 separate control (3 lines) and RGS (19 lines) expressing cell lines. All vector control lines showed similar signaling efficiency. Two RGS-expressing clones showed greater inhibition than expected from their apparent low levels of expression and were not included. To determine the relative expression levels of RGS proteins in stably transfected cell lines, cells from trypsinized plates were counted, pelleted, lysed (2 x 10^7 cells/ml) in Laemmli sample buffer and resolved by SDS-

Molecular Pharmacology Fast Forward. Published on September 27, 2007 as DOI: 10.1124/mol.107.036285
This article has not been copyedited and formatted. The final version may differ from this version.

polyacrylamide gel electrophoresis. RGS2 protein expression patterns were determined by immunoblotting using antibodies directed against the indicated epitope-tag in phosphate-buffered saline containing 0.1 % Tween-20, 3% (v/v) skim milk powder, and 3 % (v/v) bovine serum albumin (anti-GFP, 1:400; anti-myc, 1:1000) and enhanced chemiluminescence. Where indicated, densitometric quantitation of protein expression was performed using the gel analysis function of the ImageJ 1.32j software package.

Phosphoinositide Hydrolysis Assays-- Inositol phosphate accumulation in stably and transiently transfected cell lines was measured essentially as described previously (Heximer, 2004).

Intracellular calcium imaging – HEK293 cells stably transfected with the M1 muscarinic receptor were seeded at 50 % confluence on polylysine-coated #1 glass coverslips in 6-well plates prior to transfection with 1μg plasmid DNA in FuGENE 6 (Roche). After 24 hours transfection, coverslips were washed and incubated in calcium imaging buffer (11 mM glucose, 130 mM NaCl, 4.8 mM KCl, 1.2 mM $MgCl_2$, 17 mM HEPES, and 1 mM $CaCl_2$, pH 7.3) containing 5 μm fura-2 AM and 0.05% pluronic acid for 40 minutes at 37˚C. Fura-2 loaded cells were washed again and incubated for at least 10 minutes in calcium imaging buffer to allow hydrolysis of the AM ester. Coverslips were mounted in a TC1-SL25 open-bath chamber (BioScience Tools, San Diego, CA) and imaged on an Olympus BX51WI upright microscope using a 10x water-dipping objective. Excitation light was provided by a DeltaRam V monochrometer (PTI, Lawrenceville, NJ) Fluorescence imaging was performed with ImageMaster imaging software (PTI). Images

Molecular Pharmacology Fast Forward. Published on September 27, 2007 as DOI: 10.1124/mol.107.036285
This article has not been copyedited and formatted. The final version may differ from this version.

were acquired with a Photometrics Cascade 512B cooled charge-coupled device camera (Roper Scientific, Tucson, AZ). GFP and RGS2-GFP expressing cells were identified using 488 ± 5 nm excitation and selected as regions of interest (ROIs). Relative GFP fluorescence (RGS expression) and fura-2 ratiometric (intracellular calcium) was determined for each ROI was calculated as mean pixel fluorescence value following 200 ms and 100 ms exposure respectively. For fura-2 imaging, alternating excitation wavelengths (355±5/396±5 nm) were provided at ~ 1 excitation pair per second and paired images collected through a 510 ± 20-nm emission filter (Chroma Technology Corp.). Fluorescent ratio (FR) values for the image pairs were determined for ROIs selected on the basis of their GFP expression. Baseline fluorescence ratios of nonstimulated cells were collected for 30 frames prior to the addition of 200 μM carbachol. The percentage increase from baseline FR levels to the peak stimulated FR was determined specifically for low GFP or RGS2-GFP expressing cells with relative GFP fluorescence between background levels (3300 relative fluorescent units, RFU) and an upper experimental limit of 10000 RFU. Higher, expression levels provide greater (even complete) attenuation of the intracellular calcium response, however, high intracellular GFP levels result interefere with the 396 nm channel during fura-2 excitation. For technical reasons, therefore, it is important to measure fura 2 ratios in GFP-expressing cells with a RFU of <10000.

cAMP level determination- For stably transfected lines, cells ($4x10^6$ cells per well in 6-well plates) were incubated overnight in starvation medium (1% serum). Following 15 minutes preincubation with 1mM 3-isobutyl-1-methylxanthine (IBMX), cells were

Molecular Pharmacology Fast Forward. Published on September 27, 2007 as DOI: 10.1124/mol.107.036285
This article has not been copyedited and formatted. The final version may differ from this version.

stimulated with either vehicle or 100μM isoproterenol for 15 minutes. Cells were washed with phosphate buffered saline (PBS) and lysed in hypotonic lysis buffer (50 mM Tris, pH 7.5, 4 mM EDTA, plus protease inhibitors), immediately boiled and spun at 14000 rpm. After normalization with protein levels in separate controls plated at the same density, equal amounts of protein were used in a commercial cAMP RIA kit to determine cAMP concentrations.

For cAMP measurement in transiently transfected cultures, subconfluent HEK293 cells were plated on 6-well plates and transfected with constructs expressing either Gs(Q227L) (0.25 μg/well) along with RGS2 (0.5 μg/well) and type V AC (0.03 μg/well) using FuGENE6. The vector pcDNA3 (Invitrogen) was used to normalize all of the DNA concentrations to 1.28 μg/well. After 36 h of transfection, the cells were successively starved overnight in medium containing 1% fetal bovine serum, and 2h in medium devoid of serum. cAMP accumulation was measured after 15 min treatment with 1 mM IBMX as previously described (Salim *et al.*, 2003).

Confocal Fluorescence Microscopy- Polylysine-coated 25 mm circular # 1 glass coverslips containing live transfected cells were mounted in a modified Leyden chamber containing HEPES-buffered saline solution (HBSS), pH 7.4. Confocal microscopy was performed on live cells at 22 °C using an Olympus FluoView2.1 (single-wavelength) or FluoView 1000 (dual-wavelength colocalization) laser-scanning confocal microscope. Nucleolar localization was marked with Fibrillarin-HcRed (Fradkov *et al.*, 2002) while mitochondrial staining was achieved by pre-labelling cells in 25nM tetramethylrhodamine (TMRM) for 15 minutes followed by incubation in 5nM TMRM

Molecular Pharmacology Fast Forward. Published on September 27, 2007 as DOI: 10.1124/mol.107.036285
This article has not been copyedited and formatted. The final version may differ from this version.

for the duration of the image collection. Images represent single equatorial planes obtained with a 60x oil objective. Confocal images were processed with Adobe Photoshop 7.0.

Statistical Analysis: Unless otherwise stated, data was collected from triplicate wells for each experimental condition. Relative change from baseline data was collected from at least three independent experiments and presented as Means ± S.E.M. In calcium signaling experiments data was collected from n > 30 GFP or RGS2-GFP expressing individual cells. Statistically significant differences were determined by unpaired Student's t test method and a p value of < 0.05 was deemed significant. Representative immunoblots shown reflect similar results obtained in at least three separate experiments.

Molecular Pharmacology Fast Forward. Published on September 27, 2007 as DOI: 10.1124/mol.107.036285
This article has not been copyedited and formatted. The final version may differ from this version.

RESULTS

Stable expression of human RGS2 mRNA yields multiple protein products. HEK293 cell lines stably transfected with a wild type RGS2-myc construct expressed multiple RGS2 proteins (30 to 35 kDa size range) compared to empty vector controls (Figure 1A; compare *lanes wt-1* and *control*). Based on the migration of recombinant RGS2 on SDS-PAGE we predicted that the weak protein band at 34 kDa corresponded to full-length RGS2-myc, however, at least two more highly expressed bands were observed between 30-32 kDa. This multi-band RGS2 expression pattern was very different from that from cell lines stably transfected with kzRGS2-myc, a construct that was modified to include an optimized translation start consensus (Kozak consensus (Kozak, 1986); kz). KzRGS2 lines expressed a predominant protein species corresponding to the predicted size of the full-length protein (Figure 1A; compare *lanes kz-1* and *kz-2* to *wt-1*). We examined whether the altered expression pattern correlated with altered signaling function in the wtRGS2 compared to kzRGS2 cell lines. Cell lines with relatively similar expression levels of total RGS2-myc protein (kz-1, 1.0; kz-2, 3.3; and wt-1, 3.7) were used to examine whether the RGS2 expression pattern impacted its ability to attenuate $G\alpha_q$ or ACV signaling.

RGS2-mediated inhibition of $G\alpha_q$ is similar in kzRGS2- and wtRGS2-expressing lines. To determine whether changes in the RGS2 expression pattern correlated with changes in signaling function, we measured the ability of RGS2 to inhibit $G\alpha_q$ and $G\alpha_s$/AC signaling in wtRGS2 and kzRGS2 cell lines. Previously, we demonstrated that the $G\alpha_q$ inhibitory function of stably expressed RGS proteins could be compared following stimulation of

Molecular Pharmacology Fast Forward. Published on September 27, 2007 as DOI: 10.1124/mol.107.036285
This article has not been copyedited and formatted. The final version may differ from this version.

endogenous muscarinic receptors in HEK293 cells (Heximer, 2004; Heximer *et al.*, 1999). Using a similar assay system we here compared inositol phosphate accumulation in several RGS2-expressing lines. Basal and carbachol-stimulated inositol phosphate accumulation was lower in all of the RGS2-expressing compared to the control vector-containing cell lines (Figure 1B) Thus, all of the RGS2 lines studied showed signaling characteristics consistent with the expression of functional RGS2 protein. The level of RGS2-dependent inhibition of inositol phosphate signaling appeared to be dependent on the levels of total RGS2 protein expression (summed expression of all products within 30-35 kDa range) under both basal and carbachol-stimulated conditions. Specifically, compared to the control vector cell line, the two high RGS2-expressing lines, wt-1 and kz-2, inhibited the majority of carbachol-stimulated inositol phosphate accumulation, whereas the low RGS2- expressing line kz-1 showed the lowest inhibition of inositol phosphate accumulation (Figure 1B). Together, these data suggested that RGS2-mediated $G\alpha_q$ inhibition is more dependent on the total amount of RGS2 protein in the cell than on differences in its expression pattern.

RGS2-mediated inhibition of AC is higher in kzRGS2- compared to wtRGS2-expressing lines. HEK293 cells express β-adrenergic receptors that can be stimulated with isoproterenol to increase AC activity and second messenger intracellular cAMP levels. In Figure 1C, this pathway was used to determine the relative AC inhibitory activity of RGS2 in wt-1 and kz-2, the two cell lines with the most similar total RGS2 protein levels (Figure 1A). Isoproterenol stimulation of vector control and wt-1 lines resulted in similar stimulation of cAMP accumulation above baseline levels. Data from three independent

Molecular Pharmacology Fast Forward. Published on September 27, 2007 as DOI: 10.1124/mol.107.036285
This article has not been copyedited and formatted. The final version may differ from this version.

experiments showed that the wt-1 cell line contained a similarly low level of ACV inhibitory activity as the empty vector control cell line (Figure 1C). By contrast, the kz-2 cell line showed much less AC-dependent accumulation of cAMP indicating a higher level of AC inhibitory activity in these cells. Thus, in contrast to the results for $G\alpha_q$ inhibition, the inhibition of AC signaling appeared to be highly dependent on the expression of the largest protein species.

Alternative translation initiation produces four distinct RGS2 protein products. Characterization of the product expression pattern from the endogenous RGS2 gene is difficult due to the lack of antibodies that can reliably detect low levels of protein. Therefore, we constructed an expression reporter construct by cloning the complete 32 bp 5' untranslated region and sequences encoding amino acids 1-79 of *RGS2* in frame ahead of enhanced green fluorescent protein (EGFP) in the pEGFP-C1 vector. The resulting amino-terminal(NT) RGS2-GFP fusion reporter construct, NT-GFP, drove expression of the RGS2 reporter mRNA from the cytomegalovirus (CMV) promoter. Transfection of NT-GFP into HEK cells resulted in the expression of four distinct RGS2 protein products compared to nontransfected cells (Figure 2A, *arrows*). In agreement with data from stable cell lines (Figure 1), incorporation of an optimized translation initiation consensus sequence at the first in-frame methionine resulted in production of a single full-length NT-GFP protein (Fig. 2A, lane Kz).

Insertion of an optimized translation initiation consensus sequence at the beginning of the RGS2 ORF might affect the protein expression pattern by one of two different mechanisms. First, if alternative translation start site use is responsible for the

Molecular Pharmacology Fast Forward. Published on September 27, 2007 as DOI: 10.1124/mol.107.036285
This article has not been copyedited and formatted. The final version may differ from this version.

observed multi-band profile, then optimization of initiation from the most upstream initiator codon might be expected to reduce translation start from downstream initiator codons. Second, if the band pattern is due primarily to proteolytic breakdown, a pathway mediated by the position 2 glutamine in RGS2 (Bodenstein *et al.*, 2007; Yang *et al.*, 2005), then mutation of this residue to a stabilizing alanine (required for codon optimization) might stabilize the full length RGS2 protein and prevent accumulation of smaller breakdown products.

The following observations led us to focus our attention on alternative translation start site use as an explanation for this unique expression profile. Cross-species comparison of human, mouse, and rat *RGS2* mRNAs revealed the presence of four conserved in-frame AUG initiator codons that mark the beginning four putative RGS2 ORFs (ORFs1-4) corresponding to proteins initiated from amino acid positions Met1, Met5, Met16, and Met33 (Figure 2C). Notably, the relative migration rates of the four NT-GFP derived proteins (Figure 2A) were consistent with translation from four such initiator codons. Alignment of the translation initiation consensus sequence with sequences flanking each putative initiation codons indicated that the third in-frame methionine (Met16) showed the highest degree of sequence similarity to the established translation initiation consensus sequence (Figure 2B). Moreover, the third slowest migrating NT-GFP protein was expressed more much strongly than the others (Figure 2A) consistent with the possibility of strong relative translation initiation from Met16.

To determine whether the expression profile observed in Figure 2A was produced by alternative translation initiation, AUG codons at positions Met1, Met5, Met16, and

Molecular Pharmacology Fast Forward. Published on September 27, 2007 as DOI: 10.1124/mol.107.036285
This article has not been copyedited and formatted. The final version may differ from this version.

Met33 in NT-GFP were mutated to UUG (leucine) codons, and the resulting protein expression profiles compared on immunoblots. Ablation of the first two AUG codons, corresponding to Met1 and Met5, completely eliminated expression of full-length and second-most slowly migrating RGS2 bands (Figure 2D, M1L, M5L). Similarly, ablation of AUG codons at Met16(M16L) and Met33(M33L) selectively abolished expression of the third- and fourth-most slowly migrating protein bands respectively. Treatment of cells expressing NT-GFP with the proteasome inhibitor MG132 increased expression of all four products, but did not dramatically reduce the amount of smaller products suggesting that the faster migrating species were not stable byproducts of proteasome-dependent degradation (Figure 2E). To rule out the unlikely possibility that point mutations in the NT-GFP reporter construct altered the transcription rate or stability of the RGS2 mRNA, RT-PCR was performed on total RNA samples from cells transfected with the various constructs. Steady-state levels of reporter mRNAs were not different in NT-GFP and NT(M33L)-GFP transfected cells (data not shown). Therefore, data from stable cell lines and mutant NT-GFP translation reporter constructs suggest that the existence of the four protein bands can be explained by alternative translation initiation from four different initiator AUGs corresponding to amino acid positions Met1, Met5, Met16, and Met33 in the RGS2 protein.

Differential translation start site model is consistent with stable cell line signaling data. Signaling data in Figure 1 suggest that the RGS2 cDNA can produce a set of proteins that differ in their ability to inhibit AC but not $G\alpha_q$ signaling. The diagram in Figure 3 summarizes the location of the four putative initiator codons relative to known functional

Molecular Pharmacology Fast Forward. Published on September 27, 2007 as DOI: 10.1124/mol.107.036285
This article has not been copyedited and formatted. The final version may differ from this version.

domains in RGS2 (GTPase activation protein; *GAP*, and adenylyl cyclase inhibition, *AC* shown below). Figure 3A compares the predicted architecture of proteins expressed in the different stable cell lines from Figure 1, where initiation sites are shown as *gray shaded bars* with *forward-facing arrows* and labeled by to their amino acid position number relative to Met1. *Black shaded bar*s indicate optimization of a translation initiation consensus sequence. Figure 3B compares the wild type and mutant NT-GFP translation reporter constructs compared in Figure 2D. We asked whether a single unifying model could explain the relationship between the RGS2 expression pattern and its biological function? Since the kz-1 and kz-2 cell lines apparently express mainly Met1-derived protein compared to Met16-derived protein in the wt-1 line, we inferred that loss of specific sequences between Met1 and Met16 explained the observed lower adenylyl cyclase inhibition by RGS2 in wt-1 cells (Figure 1). Indeed, the Met16-derived product lacks the AC inhibitory domain (*AC*) and would be expected to show weaker inhibition of β2-adrenergic signaling than Met1-derived protein (Figure 3A). Thus, the evidence suggests that alternative translation of RGS2 can produce several RGS2 proteins with different abilities to inhibit adenylyl cyclase activity. As one test of this model is the functional characterization of each putative RGS2 open reading frame (ORF) in isolation, Figure 3C shows the design of kzORF1-4, the expression constructs used for this purpose.

AC inhibition domain is not a key modulator of RGS2 plasma membrane association. Previously we showed that the RGS2 NTD is required for its association with the plasma membrane and that amphipathic helical sequences between residues 39-52 were

Molecular Pharmacology Fast Forward. Published on September 27, 2007 as DOI: 10.1124/mol.107.036285
This article has not been copyedited and formatted. The final version may differ from this version.

necessary and sufficient for this function (Heximer *et al.*, 2001). RGS2 can also be found in plasma membrane signaling complexes containing a 7TMR (β2-adrenergic receptor), G_s, and type IV or VI adenylyl cyclase (Roy *et al.*, 2006a). Thus, it appears that there are multiple discrete domains within the RGS2 NTD that are capable of cooperatively regulating its localization and signaling function. The relative contribution of the AC-inhibition domain to membrane localization is currently unknown and may have important functional implications in cells with different RGS2 expression profiles. Since proteins driven from Met16 and Met33 lack the AC-inhibition domain, the NT-GFP and the AUG-UUG mutant constructs provided a unique opportunity to study the contribution of this domain to membrane association (Figure 4A). The four NT-GFP products were strongly localized to the plasma membrane with very little GFP fluorescence in the cytoplasm, consistent with the pattern of localization previously reported for the complete amino terminal domain (Heximer *et al.*, 2001). The combined mutation of the first two in frame AUGs in NT (M1L, M5L)-GFP, did not alter tonic plasma membrane targeting efficiency, consistent with the notion that the primary determinants for plasma membrane are located downstream of Met16 in the RGS2 amino terminus (Figure 4A). Since the AC inhibitory domain is located within amino acids Val 9 to His 11, it seems unlikely that this domain contributes to basal association of RGS2 with the plasma membrane, but rather that it is required for specific recruitment or coordination of activated Gs-coupled receptor signaling complexes following exposure to a physiologic stimulus.

Mitochondrial but not nuclear/nucleolar localization RGS2 is dependent on translation start site use. It is becoming more widely appreciated that NTD of RGS2 can interact

Molecular Pharmacology Fast Forward. Published on September 27, 2007 as DOI: 10.1124/mol.107.036285
This article has not been copyedited and formatted. The final version may differ from this version.

with an increasing number of cellular partners to coordinate localized signaling events (Heximer and Blumer, 2007). Compared to the GFP protein, which is evenly distributed throughout the cytosol and nucleus of HEK293 cells (Heximer *et al.*, 2001), the RGS2 NTD directs nucleoplasmic and possibly nucleolar localization (Figure 4A). It may be that the cell sequesters RGS2 in the nucleus to prevent its potent inhibition of signaling pathways, or that there is a specific purpose for RGS2 inside the nuclear compartment. We therefore examined its localization to identify new potential sites of RGS2 function. The NT-GFP proteins showed strong colocalization (*arrows*) with the nucleolar marker Fibrillarin-HcRed (Figure 4B) indicating a possible role for RGS2 in nucleoli. NT-GFP-derived proteins also associated with punctate organellar structures in the cytosol previously predicted to be mitochondria (Heximer *et al.*, 2001). These features were shown to precisely colocalize (*arrow heads*) with the mitochondrial-specific dye TMRM (Figure 4C). It is the only Met33–initiated protein that targets mitochondria, since TMRM colocalization was abolished for the NT(M33L)-GFP construct. It remains to be determined whether RGS2, and more specifically its Met33-derived ORF, plays a role in the regulation of mitochondrial function.

kzORF1-4 are recruited from the nucleus by $G\alpha_q$ but not $G\alpha_s$/ACV signaling. While the RGS2 NTD mediates localization and AC inhibition, the RGS2 GAP domain mediates its function as a $G\alpha_q$ inhibitor. Our group and others have shown that these protein domains cooperate to mediate recruitment of RGS2 from the nucleus in response to a $G\alpha_q$ stimulus (Heximer *et al.*, 2001; Roy *et al.*, 2003). We asked whether chronic $G\alpha_s$/ACV signaling can also recruit these four RGS2 proteins (kzORFs) out of the nucleus (Figure

Molecular Pharmacology Fast Forward. Published on September 27, 2007 as DOI: 10.1124/mol.107.036285
This article has not been copyedited and formatted. The final version may differ from this version.

5). We predicted that RGS2 proteins containing the AC inhibition domain (kzORF1 and kzORF2) would be more efficiently recruited to the plasma membrane. Expression of each RGS2 product was achieved by PCR cloning and inclusion of an optimized translation initiation sequence at the upstream AUG codon (see Figure 3C) The resulting clones were named kzORF1 through kzORF4. Each kzORF construct expressed a predominant protein band on anti-GFP immunoblots (Figure 5A). Confocal microscopy was used to examine the subcellular localization of kzORF1-4 in control cells and in cells coexpressing constitutively active $G\alpha_q$ or $G\alpha_s$/ACV (Figure 5B and C). All four kzORF clones showed efficient recruitment from the nucleus to the plasma membrane/cytosol compartment in response to $G\alpha_q$ activation (Figure 5B). By contrast, none of the different kzORF constructs tested were efficiently recruited from the nucleus to the plasma membrane/cytosol in $G\alpha_s$/ACV-stimulated cells. Relative pixel intensity values indicated that $G\alpha_q$ activation resulted in recruitment of kzORF1 from the nucleus, whereas $G\alpha_s$/ACV activation had no effect on its relative distribution, despite the presence of an intact AC inhibition domain (Figure 5C).

Taken together, the subcellular localization data for the NT-GFP and kzORF constructs do not support a role for alternative translation initiation in the differential control of RGS2 targeting to the plasma membrane or recruitment from the nucleus. Therefore, functional differences between the RGS2 ORFs are most likely to be the result of their intrinsic inability to inhibit $G\alpha_q$ or ACV.

KzORFs1-4 show similar levels of $G\alpha_q$ inhibitory function. Data from our translation reporter system and RGS2 stable lines suggest that all four RGS2 proteins produced by

Molecular Pharmacology Fast Forward. Published on September 27, 2007 as DOI: 10.1124/mol.107.036285
This article has not been copyedited and formatted. The final version may differ from this version.

alternative translation were functionally competent with respect to their $G\alpha_q$ inhibition activity. However, it was not possible to determine the relative function of the individual products because these proteins were expressed simultaneously from the wild type *RGS2* mRNA construct. First, we examined $G\alpha_q$ inhibition by each individual RGS2 ORF under chronic and acute signaling conditions. We measured the ability of kzORF1-4 to inhibit inositol phosphate accumulation in cells cotransfected with constitutively active $G\alpha_q$(R183C). Transfection of $G\alpha_q$(R183C) alone resulted in a ~50 fold increase in accumulated IPx levels relative to nontransfected HEK293 cells. Notably, $G\alpha_q$(R183C)-dependent phosphoinositide hydrolysis was attenuated to a similar extent (>80% reduction of maximum signal) by each of the different RGS2 proteins (Figures 6A). In a separate series of experiments where 3-fold less RGS2 plasmid was used, kzORF1 and kzORF3 both attenuated signaling to a similar extent (~ 40% reduction of maximal signal, data not shown). In acute assays, HEK293 cells stably expressing the M1 muscarinic receptor (M1-HEK) were used to study the function of kzORFs1-4 as inhibitors of agonist-mediated increases in intracellular calcium. Specifically, M1-HEK cells were transiently transfected with pEGFP control plasmid or the indicated RGS2 kzORF-GFP fusion construct prior to Fura 2 loading and stimulation with carbachol. The $G\alpha_q$ inhibitory function of ORFs 1-4 was determined by measuring intracellular calcium responses in single cells that had been preselected on the basis of their kzORF-GFP expression. When RGS2 activity was compared between cells expressing similar levels, the four kzORFs all showed similar inhibition of intracellular calcium elevation (~ 40 %) in response to a 200 μM carbachol bolus (Figure 6B). Taken together, these data

Molecular Pharmacology Fast Forward. Published on September 27, 2007 as DOI: 10.1124/mol.107.036285
This article has not been copyedited and formatted. The final version may differ from this version.

indicated that the four RGS2 ORFs produced by alternative translation initiation were not functionally different at the level of their $G\alpha_q$ inhibition.

Alternative RGS2 translation start sites produce functionally distinct inhibitors of AC. Data from Figure 1C suggest that the different RGS2 proteins produced by alternative translation of the *RGS2* mRNA may behave differently in their abilities to attenuate GPCR-mediated cAMP accumulation in HEK cells. We predicted that these differences were attributed to the specific loss of the AC inhibitory domain in Met16 (ORF3)- and Met33 (ORF4)-derived proteins. To determine the relative AC inhibitory potential of the various alternatively translated proteins, we used a cotransfection assay that was developed to study the function of the RGS2 as a direct inhibitor of ACV function (Salim *et al.*, 2003). The various kzORFs were transiently cotransfected with constitutively active Gs(Q227L) and ACV in HEK293 cells after which, cAMP accumulation was measured (Figure 7). In the presence of active Gs(Q227L) and ACV, steady-state intracellular cAMP levels were increased by ~20 fold compared to unstimulated controls. The coexpression of the full-length RGS2 (kzORF1) and kzORF2 proteins each resulted in a >50% decrease in cAMP levels. As predicted from the expected downstream initiator codon positions relative to the AC inhibitory domain, kzORF3 and kzORF4 were completely deficient at inhibiting cAMP accumulation by Gs(Q227L) and ACV.

Activation of $G\alpha_s$ but not $G\alpha_q$ signaling pathways alters the expression profile of RGS2 translation products. Since the above data show that the biologic activity of RGS2 depends on the relative expression levels of different proteins produced from different

Molecular Pharmacology Fast Forward. Published on September 27, 2007 as DOI: 10.1124/mol.107.036285
This article has not been copyedited and formatted. The final version may differ from this version.

translation initiation sites, we next determined whether the relative abundance of the alternative translation products was regulated by different chronic G-protein signaling conditions (Figure 8). Accordingly, the translation reporter vector, NT-GFP, was expressed alone or together with either $G\alpha_q$(R183C) or $G\alpha_s$(Q227L) and ACV. The resulting protein expression profiles were compared on immunoblots. While no changes in the RGS2 profile were observed in response to $G\alpha_q$-stimulation, coexpression of $G\alpha_s$ and ACV resulted in an increase in the expression of the Met-1 derived protein (Figure 8A). Also evident was a concurrent decrease in the expression of the Met-16 derived protein such that the ratio of Met-1 to Met-16 derived protein was greatly increased in response to $G\alpha_s$ and ACV (Figure 8B). Since the transcriptional activity of both the RGS2 and CMV promoters is increased in a cAMP-dependent manner, we asked whether the observed increase in the Met-1 derived protein was caused by transcriptional upregulation following cotransfection with $G\alpha_s$ and ACV. The NT-GFP cassette was cloned into a tetracycline-inducible vector (pREV-TRE) and the RGS2 expression profile was examined at different rates of transcription that were controlled by the amount of doxycycline added to the culture medium. Increased transcription from this reporter construct was evident from stepwise increases RGS2 protein expression, however this was not associated an increased level of the Met1-derived compared to the Met 16-derived protein (supplemental data). Moreover, the coexpression of $G\alpha_s$ and ACV resulted in increased relative expression of the Met-1 derived protein irrespective of the doxycycline concentration used. Together, these data suggest that the Met-1 derived protein is upregulated independently from cAMP-dependent changes in transcription rate.

Molecular Pharmacology Fast Forward. Published on September 27, 2007 as DOI: 10.1124/mol.107.036285
This article has not been copyedited and formatted. The final version may differ from this version.

DISCUSSION

RGS protein genes express multiple gene products with different functional properties. As completion of the human and mouse genome sequencing projects draw near, the search for novel RGS protein products with different biological functions is an emerging area of interest. Alternative mRNA splicing is a common mechanism by which several RGS proteins are produced from a single gene. Genes such as *RGS3* and *RGS12* produce alternatively spliced mRNAs that furnish their respective GAP domains with varying complements of PDZ domain or PDZ domain-binding sequences (Kehrl *et al.*, 2002; Snow *et al.*, 1998). Likewise, *RGS6*, *RGS8*, RGS9, *RGS10*, and *RGS11* yield splice variants of their GAP domain sequences with more than one complement of regulatory domains (Chatterjee *et al.*, 2003; Giudice *et al.*, 2001; Granneman *et al.*, 1998; Haller *et al.*, 2002; Saitoh *et al.*, 2002). It is intriguing that nearly all of the RGS proteins derived from alternatively spliced mRNAs contain the RGS GAP domain sequences. Thus, it appears that cells modulate their G-protein signaling profiles via alternative splicing of appropriate regulatory domains onto RGS domain sequences. It is of interest, therefore, to characterize the mechanisms for alternative RGS protein production as a step toward understanding cellular modulation of G-protein signaling.

Multiple RGS2 proteins are expressed from a single mRNA. Our analysis showed that *RGS2*, like many of the RGS protein-encoding genes, is capable of producing more than one protein product. By contrast, however, *RGS2* did not appear to use differential splicing to generate these species. Some RGS proteins (RGS2, RGS4, RGS5 and RGS16) are targeted for proteasome-mediated degradation through the N-end rule

Molecular Pharmacology Fast Forward. Published on September 27, 2007 as DOI: 10.1124/mol.107.036285
This article has not been copyedited and formatted. The final version may differ from this version.

pathway, a mechanism that is dependent on cleavage of the first methionine and the protein stabilizing/destabilizing nature of second amino acid (Bodenstein *et al.*, 2007; Davydov and Varshavsky, 2000; Hu *et al.*, 2005; Lee *et al.*, 2005). We asked whether such a mechanism could produce the observed expression profile. Our current data do not appear to support this notion. First, according to the eukaryotic N-end rule (Varshavsky, A., 1996) the Q, F, D, K residues at position 2 (see Table I) are all destabilizing residues and, therefore, should not promote selective accumulation of any of the four species. Second, the addition of the proteasome inhibitor MG132 to cells expressing NT-GFP did not selectively stabilize the full-length RGS2 band at the expense of the smaller proteins. Although we cannot rule out the possibility that some of the ORF1-4 derived proteins have a higher intrinsic stability than the others, the specific loss of single protein bands following AUG mutagenesis clearly points to alternative translation initiation as the primary explanation for the four species.

Alternative translation initiation yields RGS2 proteins with varying biologic functions. To the best of our knowledge, this is the first example of alternative translation initiation leading to the expression of RGS protein products capable of conferring different biologic activities. Indeed, the abilities of the different RGS2 products to inhibit AC were dramatically different. Consistent with their lack of an AC inhibitory domain, kzORF3 and kzORF4 were deficient of AC inhibitory function. These data provide supporting evidence for the notion that alternative translation start site initiation is another potential mechanism for the regulation of RGS protein function in mammalian cells. It will be of interest to determine whether these alternatively translated proteins are

Molecular Pharmacology Fast Forward. Published on September 27, 2007 as DOI: 10.1124/mol.107.036285
This article has not been copyedited and formatted. The final version may differ from this version.

capable of differentially regulating other recently identified RGS2 effectors such as TRPV6 for which the interaction domain in RGS2 amino terminus is not known.

Leaky ribosome scanning promotes alternative translation initiation of RGS2. Our data support the use of four different initiation codons in the *RGS2* mRNA and predict that a number of ribosomes are able to bypass the upstream initiator codon(s) in the wild type *RGS2* mRNA. Three mechanisms have been proposed to explain how translation from multiple ORFs in a single mRNA is achieved: 1) internal ribosome entry; 2) ribosome shunting; and 3) leaky ribosome scanning (Kozak, 1991). Internal ribosome entry has been described for a number of genes including c-myc, and the p58 and p110 PITSLRE protein kinases (Cornelis *et al.*, 2000; Nanbru *et al.*, 1997). Inclusion of a strong translation initiation signal at the first in-frame AUG codon resulted in loss of expression of the other smaller RGS2 products. While this mutant also incorporates a stabilizing alanine residue at the second amino acid position that could increase its relative stability compared to the other ORFs, this mechanism cannot explain the loss of expression of the other products. Moreover, the loss of specific protein bands in the M>L mutagenesis experiments suggests that translation start site usage is the primary factor controlling the observed change in expression pattern.

What is the mechanism controlling differential translation start site use in the RGS2 cDNA? Ablation of downstream ORF initiation in the RGS2-myc cell lines and the cells expressing the NT-GFP reporter argues strongly against the possibility that the *RGS2* mRNA contains one or more strong IRES elements. At present we cannot rule

ribosome shunting on the *RGS2* mRNA, a mechanism where ribosomes are repositioned across strong RNA hairpins. However, this mechanism requires termination of translation of the upstream ORF and reinitiation of the shunted ribosomes (Hemmings-Mieszczak *et al.*, 2000). Clearly the multiple RGS2 ORFs in question are long overlapping sequences that would make a termination/reinitiation event via ribosome shunting highly improbable.

In the ribosome scanning model of translation, the 43 S ribosomal complex scans the 5'-UTR in a 5' to 3' direction until it reaches an AUG within the context of a good consensus initiation sequence, where translation begins. Leaky ribosome scanning can produce multiple protein products if the translation machinery does not efficiently recognize the upstream initiator codons. To date, only a small subset of cellular mRNAs has been reported to express protein products from more than one start codon. Among these are C/EBPα and C/EBPβ that each give rise to multiple products because of weak translation initiation consensus sequences at their upstream AUG codons (Calkhoven *et al.*, 2000). One predicted consequence of the leaky scanning model is that initiation from downstream AUG codons should increase if upstream alternative start sites are disrupted. Indeed, our studies with the NT-GFP translational reporter show that this occurs in the *RGS2* mRNA since disruption of the initiator sequence for the strongly recognized AUG codon for Met16 results in increased expression of the Met33-derived protein. Thus, it appears likely that *RGS2* can be added to this small set of genes whose protein expression profile is mediated by leaky ribosome scanning.

Molecular Pharmacology Fast Forward. Published on September 27, 2007 as DOI: 10.1124/mol.107.036285
This article has not been copyedited and formatted. The final version may differ from this version.

G-protein signaling status regulates the RGS2 protein expression profile. *RGS2* gene expression is highly tuned to the signaling status of the cell. *RGS2* is an immediate-early gene whose mRNA levels are increased in a number of cell types in response to stimuli that increase intracellular calcium and cAMP (Kehrl and Sinnarajah, 2002). Thus, it has been proposed that *RGS2* mRNA levels may be increased as part of a negative feedback mechanism to reciprocally modulate $G\alpha_q$- and AC-dependent signaling (Roy *et al.*, 2006b). The current study suggests that the regulation of posttranscriptional events may be equally important for integrating signaling feedback loops. Specifically, chronic $G\alpha_s$ signaling increased expression of the Met1-derived compared to the Met16-derived protein, an observation consistent with signaling-dependent modulation of translation efficiency at Met1. Notably, in forskolin-treated osteoblasts, the largest RGS2 protein is also apparently expressed at much higher levels than the other proteins suggesting that a similar regulatory mechanism may be present in other cell types and tissues (Roy *et al.*, 2006b). The precise mechanism for this unique type of regulation, however, remains to be determined. Nonetheless, this unique adaptation of the RGS2 expression profile to a change cell signaling status represents a new type of signaling feedback mechanism that implicates regulated alternative translation start site use in the regulation of G-protein coupled signaling.

Molecular Pharmacology Fast Forward. Published on September 27, 2007 as DOI: 10.1124/mol.107.036285
This article has not been copyedited and formatted. The final version may differ from this version.

FOOTNOTES

We gratefully acknowledge the technical support of Janet He and Ashley Misquitta.

Molecular Pharmacology Fast Forward. Published on September 27, 2007 as DOI: 10.1124/mol.107.036285
This article has not been copyedited and formatted. The final version may differ from this version.

REFERENCES

Berman, D. M., Wilkie, T. M., and Gilman, A. G. (1996). GAIP and RGS4 are GTPase-activating proteins for the Gi subfamily of G protein alpha subunits. Cell *86*, 445-452.

Bernstein, L. S., Ramineni, S., Hague, C., Cladman, W., Chidiac, P., Levey, A. I., and Hepler, J. R. (2004). RGS2 binds directly and selectively to the M1 muscarinic acetylcholine receptor third intracellular loop to modulate Gq/11alpha signaling. J Biol Chem *279*, 21248-56. Epub 2004 Feb 19.

Bodenstein, J., Sunahara, R. K., and Neubig, R. R. (2007). N-terminal residues control proteasomal degradation of RGS2, RGS4, and RGS5 in HEK293 cells. Mol Pharmacol *12*, 12.

Calkhoven, C. F., Muller, C., and Leutz, A. (2000). Translational control of C/EBPalpha and C/EBPbeta isoform expression. Genes Dev *14*, 1920-32.

Chatterjee, T. K., Liu, Z., and Fisher, R. A. (2003). Human RGS6 gene structure, complex alternative splicing, and role of N terminus and G protein gamma-subunit-like (GGL) domain in subcellular localization of RGS6 splice variants. J Biol Chem *278*, 30261-71. Epub 2003 May 21.

Cornelis, S., Bruynooghe, Y., Denecker, G., Van Huffel, S., Tinton, S., and Beyaert, R. (2000). Identification and characterization of a novel cell cycle-regulated internal ribosome entry site. Mol Cell *5*, 597-605.

Davydov, I. V., and Varshavsky, A. (2000). RGS4 is arginylated and degraded by the N-end rule pathway in vitro. J Biol Chem *275*, 22931-41.

Fradkov, A. F., Verkhusha, V. V., Staroverov, D. B., Bulina, M. E., Yanushevich, Y. G., Martynov, V. I., Lukyanov, S., and Lukyanov, K. A. (2002). Far-red fluorescent tag for protein labelling. Biochem J *368*, 17-21.

Giudice, A., Gould, J. A., Freeman, K. B., Rastan, S., Hertzog, P., Kola, I., and Iannello, R. C. (2001). Identification and characterization of alternatively spliced murine Rgs11 isoforms: genomic structure and gene analysis. Cytogenet Cell Genet *94*, 216-24.

Granneman, J. G., Zhai, Y., Zhu, Z., Bannon, M. J., Burchett, S. A., Schmidt, C. J., Andrade, R., and Cooper, J. (1998). Molecular characterization of human and rat RGS 9L, a novel splice variant enriched in dopamine target regions, and chromosomal localization of the RGS 9 gene. Mol Pharmacol *54*, 687-94.

Hague, C., Bernstein, L. S., Ramineni, S., Chen, Z., Minneman, K. P., and Hepler, J. R. (2005). Selective inhibition of alpha1A-adrenergic receptor signaling by RGS2 association with the receptor third intracellular loop. J Biol Chem. *280*, 27289-95. Epub 2005 May 24.

Haller, C., Fillatreau, S., Hoffmann, R., and Agenes, F. (2002). Structure, chromosomal localization and expression of the mouse regulator of G-protein signaling10 gene (mRGS10). Gene *297*, 39-49.

Hemmings-Mieszczak, M., Hohn, T., and Preiss, T. (2000). Termination and peptide release at the upstream open reading frame are required for downstream translation on synthetic shunt-competent mRNA leaders. Mol Cell Biol *20*, 6212-23.

Heo, K., Ha, S. H., Chae, Y. C., Lee, S., Oh, Y. S., Kim, Y. H., Kim, S. H., Kim, J. H., Mizoguchi, A., Itoh, T. J., Kwon, H. M., Ryu, S. H., and Suh, P. G. (2006). RGS2 promotes formation of neurites by stimulating microtubule polymerization. Cell Signal. *18*, 2182-92. Epub 2006 May 23.

Heximer, S. P. (2004). RGS2-mediated regulation of Gqalpha. Methods Enzymol *390*, 65-82.

Heximer, S. P., and Blumer, K. J. (2007). RGS proteins: Swiss army knives in seven-transmembrane domain receptor signaling networks. Sci STKE. *2007*, pe2.

Heximer, S. P., Lim, H., Bernard, J. L., and Blumer, K. J. (2001). Mechanisms governing subcellular localization and function of human RGS2. J Biol Chem *276*, 14195-203.

Heximer, S. P., Srinivasa, S. P., Bernstein, L. S., Bernard, J. L., Linder, M. E., Hepler, J. R., and Blumer, K. J. (1999). G protein selectivity is a determinant of RGS2 function. J Biol Chem *274*, 34253-9.

Hu, R. G., Sheng, J., Qi, X., Xu, Z., Takahashi, T. T., and Varshavsky, A. (2005). The N-end rule pathway as a nitric oxide sensor controlling the levels of multiple regulators. Nature. *437*, 981-6.

Ingi, T., Krumins, A. M., Chidiac, P., Brothers, G. M., Chung, S., Snow, B. E., Barnes, C. A., Lanahan, A. A., Siderovski, D. P., Ross, E. M., Gilman, A. G., and Worley, P. F. (1998). Dynamic regulation of RGS2 suggests a novel mechanism in G-protein signaling and neuronal plasticity. J Neurosci *18*, 7178-88.

Kehrl, J. H., and Sinnarajah, S. (2002). RGS2: a multifunctional regulator of G-protein signaling. Int J Biochem Cell Biol. *34*, 432-8.

Kehrl, J. H., Srikumar, D., Harrison, K., Wilson, G. L., and Shi, C. S. (2002). Additional 5' exons in the RGS3 locus generate multiple mRNA transcripts, one of which accounts for the origin of human PDZ-RGS3. Genomics *79*, 860-8.

Kozak, M. (1986). Point mutations define a sequence flanking the AUG initiator codon that modulates translation by eukaryotic ribosomes. Cell *44*, 283-92.

Kozak, M. (1991). An analysis of vertebrate mRNA sequences: intimations of translational control. J Cell Biol *115*, 887-903.

Lee, M. J., Tasaki, T., Moroi, K., An, J. Y., Kimura, S., Davydov, I. V., and Kwon, Y. T. (2005). RGS4 and RGS5 are in vivo substrates of the N-end rule pathway. Proc Natl Acad Sci U S A. *102*, 15030-5. Epub 2005 Oct 10.

Ma, P., and Zemmel, R. (2002). Value of novelty? Nat Rev Drug Discov *1*, 571-2.
Nanbru, C., Lafon, I., Audigier, S., Gensac, M. C., Vagner, S., Huez, G., and Prats, A. C. (1997). Alternative translation of the proto-oncogene c-myc by an internal ribosome entry site. J Biol Chem *272*, 32061-6.

Ross, E. M., and Wilkie, T. M. (2000). GTPase-activating proteins for heterotrimeric G proteins: regulators of G protein signaling (RGS) and RGS-like proteins. Annu Rev Biochem *69*, 795-827.

Roy, A. A., Baragli, A., Bernstein, L. S., Hepler, J. R., Hebert, T. E., and Chidiac, P. (2006a). RGS2 interacts with Gs and adenylyl cyclase in living cells. Cell Signal. *18*, 336-48. Epub 2005 Aug 10.

Roy, A. A., Lemberg, K. E., and Chidiac, P. (2003). Recruitment of RGS2 and RGS4 to the plasma membrane by G proteins and receptors reflects functional interactions. Mol Pharmacol *64*, 587-93.

Roy, A. A., Nunn, C., Ming, H., Zou, M. X., Penninger, J., Kirshenbaum, L. A., Dixon, S. J., and Chidiac, P. (2006b). Up-regulation of endogenous RGS2 mediates cross-desensitization between Gs and Gq signaling in osteoblasts. J Biol Chem. *281*, 32684-93. Epub 2006 Sep 1.

Saitoh, O., Murata, Y., Odagiri, M., Itoh, M., Itoh, H., Misaka, T., and Kubo, Y. (2002). Alternative splicing of RGS8 gene determines inhibitory function of receptor type-specific Gq signaling. Proc Natl Acad Sci U S A *99*, 10138-43. Epub 2002 Jul 10.

Salim, S., Sinnarajah, S., Kehrl, J. H., and Dessauer, C. W. (2003). Identification of RGS2 and type V adenylyl cyclase interaction sites. J Biol Chem *278*, 15842-9.

Schoeber, J. P., Topala, C. N., Wang, X., Diepens, R. J., Lambers, T. T., Hoenderop, J. G., and Bindels, R. J. (2006). RGS2 inhibits the epithelial Ca2+ channel TRPV6. J Biol Chem. *281*, 29669-74. Epub 2006 Aug 8.

Sinnarajah, S., Dessauer, C. W., Srikumar, D., Chen, J., Yuen, J., Yilma, S., Dennis, J. C., Morrison, E. E., Vodyanoy, V., and Kehrl, J. H. (2001). RGS2 regulates signal transduction in olfactory neurons by attenuating activation of adenylyl cyclase III. Nature *409*, 1051-5.

Snow, B. E., Hall, R. A., Krumins, A. M., Brothers, G. M., Bouchard, D., Brothers, C. A., Chung, S., Mangion, J., Gilman, A. G., Lefkowitz, R. J., and Siderovski, D. P. (1998). GTPase activating specificity of RGS12 and binding specificity of an alternatively spliced PDZ (PSD-95/Dlg/ZO-1) domain. J Biol Chem *273*, 17749-55.

Varshavsky, A. (1996). The N-end rule: functions, mysteries, uses. Proc Natl Acad Sci USA 93(22):12142-9

Wang, X., Zeng, W., Soyombo, A. A., Tang, W., Ross, E. M., Barnes, A. P., Milgram, S. L., Penninger, J. M., Allen, P. B., Greengard, P., and Muallem, S. (2005). Spinophilin regulates Ca2+ signalling by binding the N-terminal domain of RGS2 and the third intracellular loop of G-protein-coupled receptors. Nat Cell Biol. *7*, 405-11. Epub 2005 Mar 27.

Watson, N., Linder, M. E., Druey, K. M., Kehrl, J. H., and Blumer, K. J. (1996). RGS family members: GTPase-activating proteins for heterotrimeric G-protein alpha-subunits. Nature *383*, 172-5.

Yang, J., Kamide, K., Kokubo, Y., Takiuchi, S., Tanaka, C., Banno, M., Miwa, Y., Yoshii, M., Horio, T., Okayama, A., Tomoike, H., Kawano, Y., and Miyata, T. (2005). Genetic variations of regulator of G-protein signaling 2 in hypertensive patients and in the general population. J Hypertens. *23*, 1497-505.

Zheng, B., De Vries, L., and Gist Farquhar, M. (1999). Divergence of RGS proteins: evidence for the existence of six mammalian RGS subfamilies. Trends Biochem Sci *24*, 411-4.

Molecular Pharmacology Fast Forward. Published on September 27, 2007 as DOI: 10.1124/mol.107.036285
This article has not been copyedited and formatted. The final version may differ from this version.

FOOTNOTES

This work was supported by grants from the Ontario Heart & Stroke Foundation (S.P.H., NA 5291), Parkinson's Disease Society of Canada (S.P.H., Pilot Grant Program), Canada Research Chairs Program of the Canadian Institute for Health Research (S.P.H.), the National Institutes of Health (C.W.D., GM60419; K.J.B., GM44592) and Pfizer/Washington University Biomedical Research Agreement (K.J.B.).

Molecular Pharmacology Fast Forward. Published on September 27, 2007 as DOI: 10.1124/mol.107.036285
This article has not been copyedited and formatted. The final version may differ from this version.

FIGURE LEGENDS:

Fig. 1. Comparison of protein expression profile and function of wtRGS2 and kzRGS2. *A.* HEK293 cells stably transfected with wild-type RGS2 constructs express multiple protein species compared to cells transfected with Kozak-optimized RGS2 cDNAs. Western blot analysis of total cell lysates from control, wtRGS2-$(myc)_3$ (*wt-1*) and 2 different kzRGS2-$(myc)_3$ expressing HEK293 stable lines (*kz-1* and *kz-2*). Proteins were separated on 12% Laemmli gels and characterized by immunoblotting. *Bracket* indicates the region of the gel in which the full length and various alternative RGS2 products are found to migrate. Protein expression levels for each cell line were determined as total RGS2 expression within the *bracket* region and are expressed relative to kz-1 line. * indicate the position of cross-reacting proteins observed in all HEK lysates. *B.* Basal and carbachol-stimulated inositol phosphate production in *control*, *wt-1*, *kz-1* and *kz-2* lines described in *A* above. Cells were labeled overnight with [^{3}H]-myoinositol, and treated with either water (*control*) or 200 μM carbachol (*Carb*) in the presence of 10 mM LiCl. Inositol phosphate (IPx) levels were measured 45 min after treatment. *Upper panel* shows IPx values expressed as the mean percentages (soluble IPx /total soluble inositol-containing material) of triplicate samples. Data are representative of three independent experiments. *Lower panel* shows IPx production data expressed relative to the IPx values for water-treated control in each experiment. Data are the mean of three independent experiments. S.E. are indicated by *error bars*. *C.* Basal and isoproterenol-stimulated cAMP accumulation in *control*, *wt-1* and *kz-2* lines. Cells were treated with 1mM IBMX prior to treatment with water (*Control*) or 100 μM isoproterenol (*Iso*) for 15 minutes. *Upper panel* shows cAMP accumulation in the different lines expressed as the

Molecular Pharmacology Fast Forward. Published on September 27, 2007 as DOI: 10.1124/mol.107.036285
This article has not been copyedited and formatted. The final version may differ from this version.

average amount of cAMP accumulated in duplicate samples. Data are representative of three independent experiments. *Error bars* represent the range of cAMP values for each cell line. *Lower panel* shows the average accumulation of isoproterenol-stimulated cAMP levels in the *wt-1* and *kz-2* relative to the *control* cell line. Data are from three independent experiments. S.E. are indicated by *error bars*. * $p<0.05$

Fig. 2. Comparison of wild type RGS2 translation reporter protein profiles with predicted AUG initiation sites in the *RGS2* mRNA. *A.* Translation reporter expression pattern of the NT-GFP construct. HEK cells (0.5×10^6 cells in 6 well plates) were transfected with either the wild type (*WT*) or Kozak-optimized (*KZ*) RGS2 translation initiation reporter construct NT-GFP for 24 hrs before total cell lysates were examined for RGS2-GFP expression by immunoblotting. *Arrows* indicate the position four bands that are specifically labeled by a polyclonal rabbit anti-GFP antibody (1:400 dilution) in transfected compared to nontransfected cells (--). *B.* Comparison of putative initiator codons with the optimal translation initiation (Kozak) sequence. Sequences flanking each of four potential initiator codons are aligned with the optimal translation initiation (Kozak) sequence (above). Similarity to the consensus is indicated by *shading.* The relative position of the initiator codon with respect to the first in frame methionine (Met 1) is indicated. *C.* Alignment of RGS2 mRNA sequences for rat, mouse and human genes. Putative AUG initiator codons are indicated (*UPPERCASE)* and those that are conserved in all sequences are marked (*underlined*). *D.* Analysis of putative AUG initiator codon use by site-directed mutagenesis of the NT-GFP construct. HEK cultures were transfected as above with the wild type NT-GFP construct or constructs containing

Molecular Pharmacology Fast Forward. Published on September 27, 2007 as DOI: 10.1124/mol.107.036285
This article has not been copyedited and formatted. The final version may differ from this version.

AUG to UUG mutations corresponding to amino acid changes at Met1 (*M1L*), Met5(*M5L*), Met16 (*M16L*) and Met33(*M33L*). Expression profiles were analyzed by immunoblotting as described above. *E.* Proteasome inhibition does not alter the NT-GFP expression pattern. Cells expressing wild type or mutant NT-GFP were treated with 10 μM MG132 for 5 hr prior to harvesting for immunoblotting as above.

Fig. 3. Schematic representation of cDNA expression constructs showing predicted protein products and domain structures. Predicted RGS2 protein products expressed from cDNA constructs for: (*A*) myc epitope-tagged proteins used in stable cell lines; (*B*) wild type and mutant NT-GFP translation initiation reporter; and (*C*) Kozak (kz) optimized full-length open reading frames (kzORFs). All of the predicted protein translation initiation sites are indicated by arrows and amino acid numbers above their corresponding AUG codons shaded in dark grey. Amino acid positions and ORF numbers are indicated relative to the full-length protein sequence(Accession #NP002914). In cases where initiation codons have been optimized with a Kozak consensus sequence, the shaded AUG codon is highlighted with black. The position of functional domains and protein sequence tags relative to the predicted translation initiation sites are shown below. These are denoted as follows: AC inhibitory domain (*AC*); plasma membrane targeting sequence (*PM*); GTPase activating protein or RGS core domain (*GAP*). The 5' untranslated region of the endogenous RGS2 mRNA has been incorporated into the NT-GFP reporter construct series and is shown above as *5' UTR.* Type and locations of the epitope-tags are indicated above the appropriate construct

Molecular Pharmacology Fast Forward. Published on September 27, 2007 as DOI: 10.1124/mol.107.036285
This article has not been copyedited and formatted. The final version may differ from this version.

sets and are indicated as follows: green fluorescent protein (*GFP*) and triple myc epitope tag (*3 x myc*).

Fig. 4. Subcellular localization of RGS2 amino terminal domains produced from wild type and mutant translation initiation reporter constructs. *A.* Localization of wild type and indicated NT-GFP mutation constructs were analyzed in transfected living HEK cells using confocal microscopy. Pictures are of cells with low-medium relative fluorescence and are representative of at least 50 cells transfected with the same construct. Confocal pictures were taken of HEK cells transfected with NT-GFP. Shown are GFP images collected from the basal region of the cell as determined by a *z* axis series. *B.* Colocalization of NT-GFP constructs with nucleolar markers in live cells. HEK cells were cotransfected with wild type NT-GFP and the nucleolar marker protein fibrillarin (Fibrillarin-HcRed). Using different lasers for excitation (488 nm, GFP; 543 nm, HcRed) and emission spectrum discrimination capabilities of the Olympus FV1000 confocal microscope, green- and red-channel images were collected from the same confocal plane to determine the subcellular localization of NT-GFP and Fibrillarin-HcRed respectively. Merged images were created to demonstrate the extent of colocalization (yellow) of these constructs. *C.* Colocalization of NT-GFP constructs with mitochondrial dyes in live cells. HEK cells transfected with the wild type or M33L NT-GFP constructs were incubated in the mitochondrial targeted fluorescent dye TMRM. Colocalization was determined as in *B.*

Molecular Pharmacology Fast Forward. Published on September 27, 2007 as DOI: 10.1124/mol.107.036285
This article has not been copyedited and formatted. The final version may differ from this version.

Fig. 5. Effect of GAP domain function and G-protein-signaling status on RGS2 localization determinants.

A. Western blot of total cell lysate from cells transfected with the specified construct shows that the presence of a Kozak consensus sequence results in the production of only one protein species. *B.* Localization of the indicated RGS2 kzORF-GFP fusion constructs with and without either constitutively active $G\alpha_q$(*Gq**) or $G\alpha_s$ and ACV(*(Gs*)/ACV*) was examined in transiently transfected cells as described above. *C.* The ratio of GFP signal between the nucleus and plasma membrane was measured using ImageJ. Shown are means +/- S.E.M.

Fig. 6. Analysis of $G\alpha_q$ inhibitory potential of the different RGS2 kzORF-derived products. *A.* HEK cells were cotransfected with constitutive $G\alpha_q$ (*Gq**) and control plasmid DNA, with and without the indicated RGS2 kzORF expression plasmids. Total DNA in each transfection was 6μg. Triplicate wells containing cells (~$1x10^6$) were incubated in the presence of [^{3}H]-myoinositol and 10mM LiCl. Inositol phosphate levels were assayed as described in 'Experimental Procedures'. *B.* M1-HEK cells on coverslips were transiently transfected with the indicated construct and loaded with fura-2 AM. Transfected cells identified as low fluorescence intensity (< 10000 relative fluorescence units) were selected for analysis of their intracellular calcium responsiveness to carbachol. Changes in intracellular calcium levels were recorded as changes in fluorescence ratio [FR= (emission at 510 nm upon excitation at 355 nm)/(emission at 510

nm upon excitation at 396 nm)]. Shown are mean FR trace values (n > 50 kinetic cells) expressing YFP control, RGS2 and RGS5 in a typical experiment showing baseline and relative FR change following addition of 100 μM carbachol (arrow). Peak relative increases in intracellular calcium levels for each cell were calculated as: Percent FR increase above baseline =[(peak stimulated FR/ unstimulated baseline FR) - 1] x 100%. Experiments show mean Percent FR increase above baseline ± S.E.M. for n > 30 cells.

Fig. 7. Inhibition of cAMP accumulation by the different RGS2 kzORF-derived proteins. Production of cAMP was measured in HEK293 cells transiently transfected as indicated with ACV (*ACV*), Gs*, and the kzORF derived proteins (*kzORF1-4*). Data are expressed as mean +/- SE from a single experiment and are representative of three experiments each performed in duplicate. * denotes a significant decrease in Gs*/ACV stimulated cAMP levels ($p < 0.05$) for the indicated kzORF constructs compared to control lane (with no RGS construct).

Fig. 8. Characterization of the RGS2 expression profile under different G-protein signaling conditions. *A.* Profile of NT-GFP expression in cells with chronic $G\alpha_s$ or $G\alpha_q$ signaling. Cells were cotransfected with NT-GFP, and either activated $G\alpha_q$ (*Gq**) or activated $G\alpha_s$ (*Gs**)and ACV (*ACV*). Lysates were analyzed by immunoblotting with the GFP antibody as described in the legend of Fig. 2. *B.* Densitometric analysis of the relative expression of the Met1-derived and Met16-derived effect of initiation codon mutations on NT-GFP reporter plasmid expression profile in the presence and absence of

Molecular Pharmacology Fast Forward. Published on September 27, 2007 as DOI: 10.1124/mol.107.036285
This article has not been copyedited and formatted. The final version may differ from this version.

constitutive Gs/ACV signaling. The indicated mutants were cotransfected with Gs* and ACV and the expression profiles compared as in *A*. * denotes $p < 0.001$.

Molecular Pharmacology Fast Forward. Published on September 27, 2007 as DOI: 10.1124/mol.107.036285
This article has not been copyedited and formatted. The final version may differ from this version.

TABLES

Table I*: Amino terminal sequence of ORF 1-4 derived from human RGS2 gene*. The first 14 aa of each predicted RGS2 ORF is shown. Amino acid positions correspond to the full length protein sequence (Accession # NP_002914). Second position residues Q, L, D, K of each ORF are highlighted with *bold font.*

1 M	**Q**	S	A	M	F	L	A	V	Q	H	D	C	R 14	ORF1
4 M	**L**	A	V	Q	H	D	C	R	P	M	M	D	K 17	ORF2
16 M	**D**	K	S	A	G	S	G	H	K	S	E	E	K 29	ORF3
33 M	**K**	R	T	L	L	K	D	W	K	T	R	L	S 46	ORF4

Figure 1

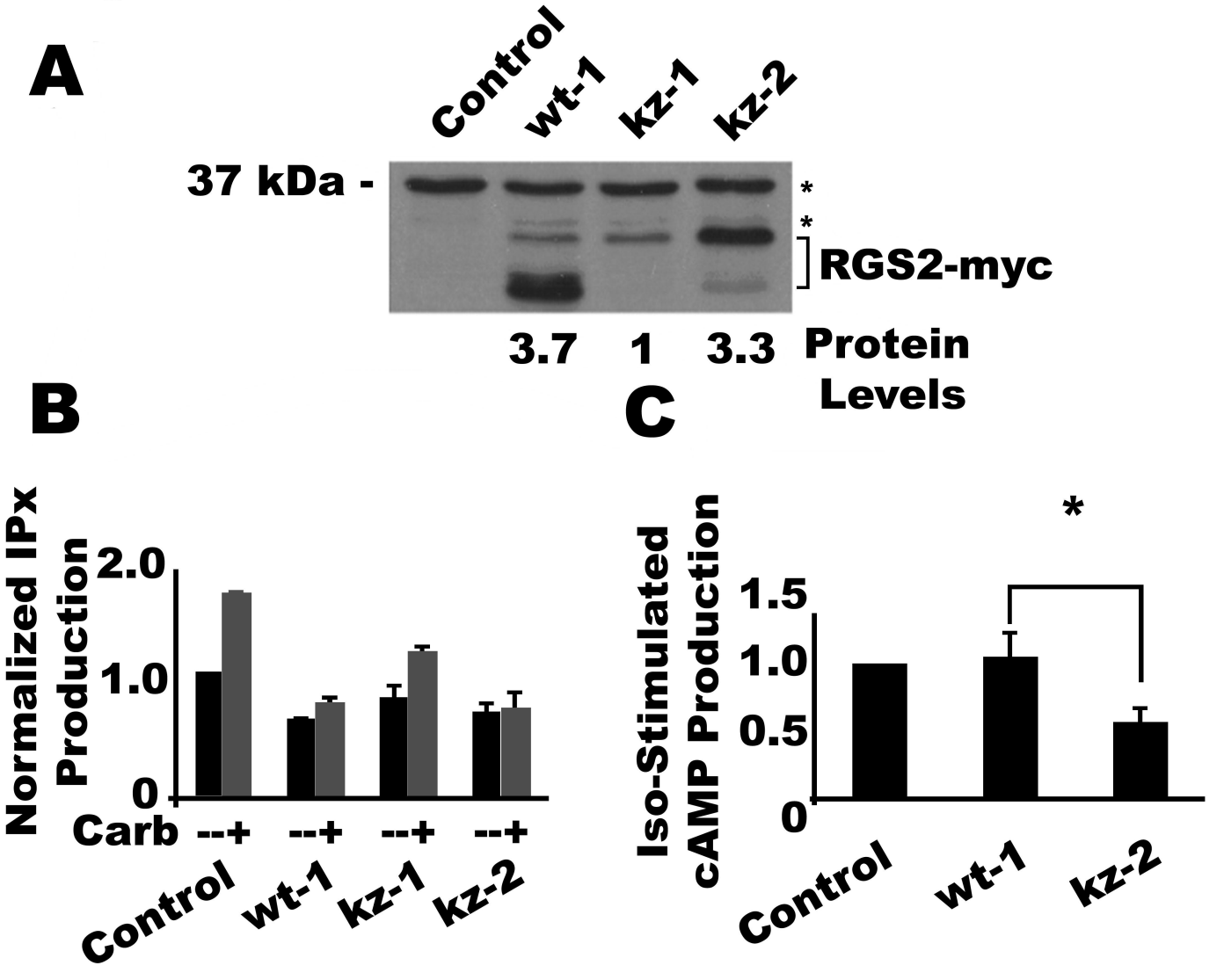
A
Control
wt-1
kz-1
kz-2
37 kDa -
*
*
RGS2-myc
3.7
1
3.3
Protein Levels
B
Normalized IPx Production
2.0
1.0
0
Carb --+ --+ --+ --+
Control
wt-1
kz-1
kz-2
C
Iso-Stimulated cAMP Production
*
1.5
1.0
0.5
0
Control
wt-1
kz-2

Figure 2

A

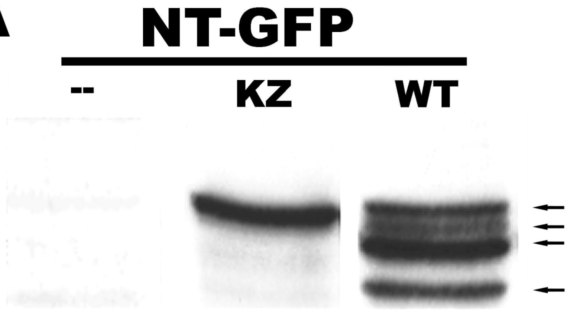

B

```
 -9    -6    -3    +1    +4            initiator
 G C C G C C A C C A U G C         ORF  pos.#

 24  a g a a A g A u a A U G c  36   1   Met 1
 37  c a a a g u g C u A U G u  49   2   Met 5
 69  u g C a g a c C C A U G G  81   3   Met 16
120  c g a g a a A a g A U G a 132   4   Met 33
```

C

```
Human [NH_002923]    1      aaaacagccggggcuccagcgggagaacgaua  32
Mouse [NH_009061.2]  1     cgaaacagcugcgguggccgcgggagucugaga  33
Rat   [NH_053453.1]  1                          cgggugucugaga  13

 33  AUGcaaagugcuAUGuucuuggcuguucaacacgacugcagacccAUGgacaaga  87
 34  AUGcaaagugccAUGuuccuggcuguccagcacgacugcguacccAUGgacaaga  88
 14  AUGcaaagugccAUGuuccuggcuguccagcacgacugcguacccAUGgacaaga  68

 88  gcgcaggcaguggccacaagagcgaggagaagcgagaaaagAUGaaacggacccu  143
 89  gugcaggcaacggccccaaggucgaggagaagcgggagaaaAUGaagcggacacu  144
 69  gcgcaggcaacggccccaaggucgaggagaagcgggagaaaAUGaagcggacacu  123
```

D

E

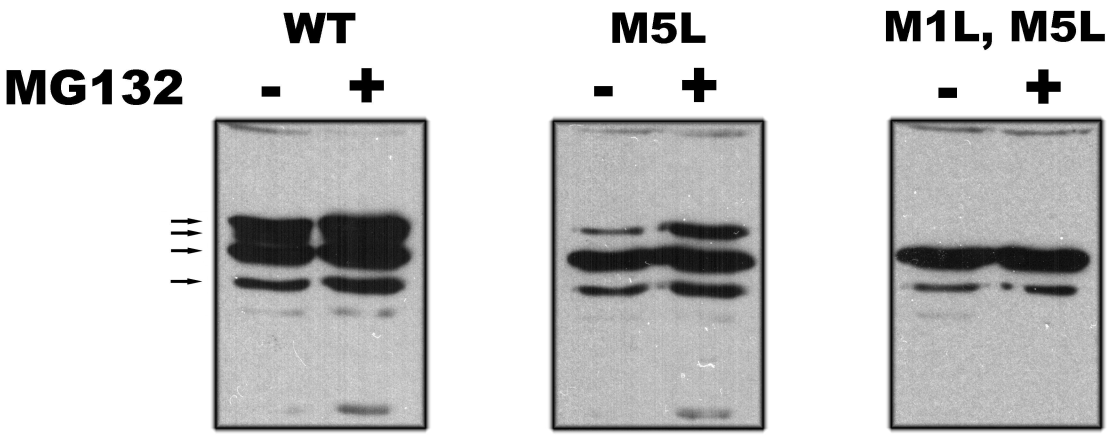

Figure 3

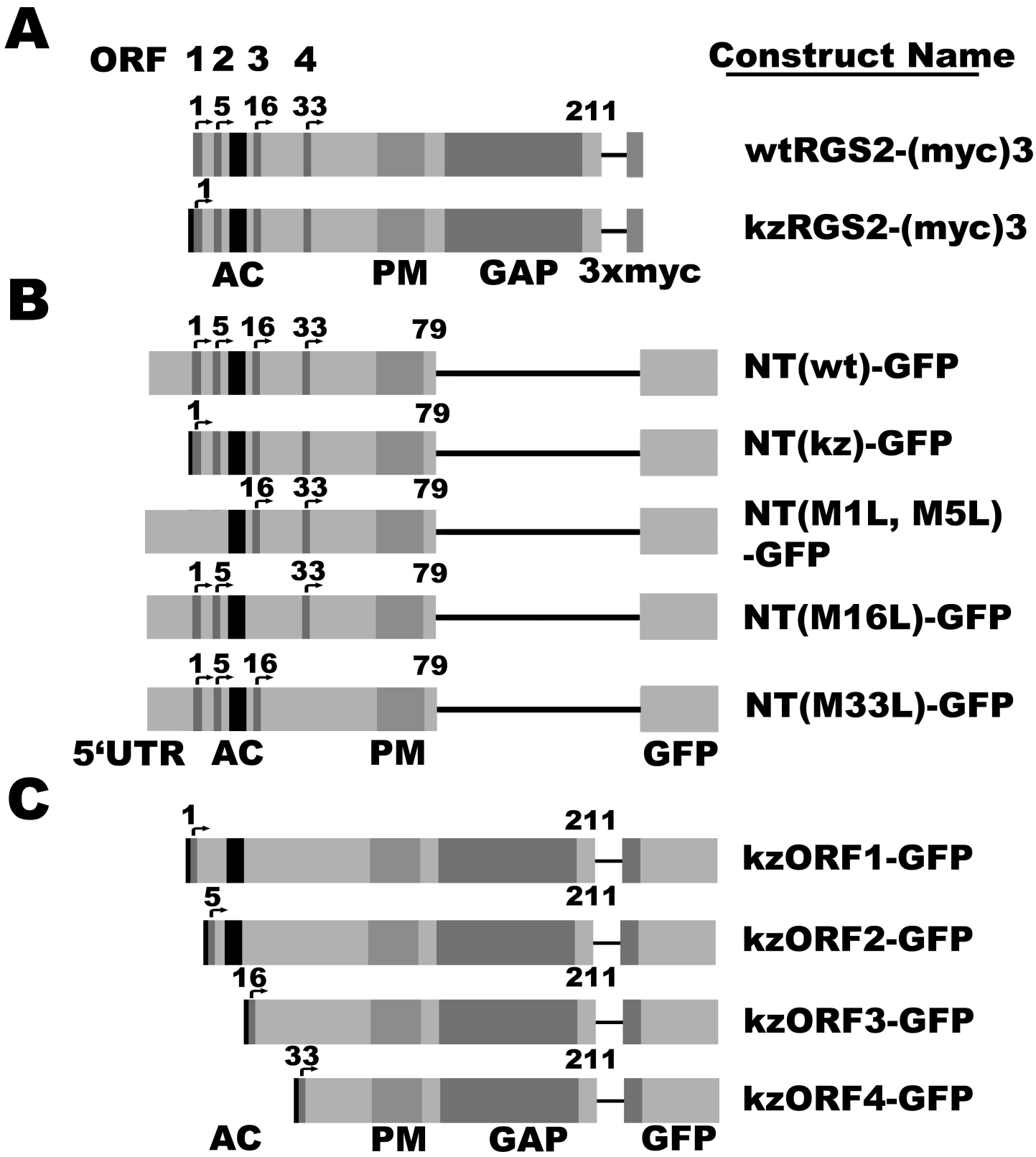
A
ORF 1 2 3 4
Construct Name
1 5 16 33
211
wtRGS2-(myc)3
1
kzRGS2-(myc)3
AC
PM
GAP
3xmyc
B
1 5 16 33
79
NT(wt)-GFP
1
79
NT(kz)-GFP
16 33
79
NT(M1L, M5L)
-GFP
1 5
33
79
NT(M16L)-GFP
1 5 16
79
NT(M33L)-GFP
5'UTR
AC
PM
GFP
C
1
211
kzORF1-GFP
5
211
kzORF2-GFP
16
211
kzORF3-GFP
33
211
kzORF4-GFP
AC
PM
GAP
GFP

Figure 4

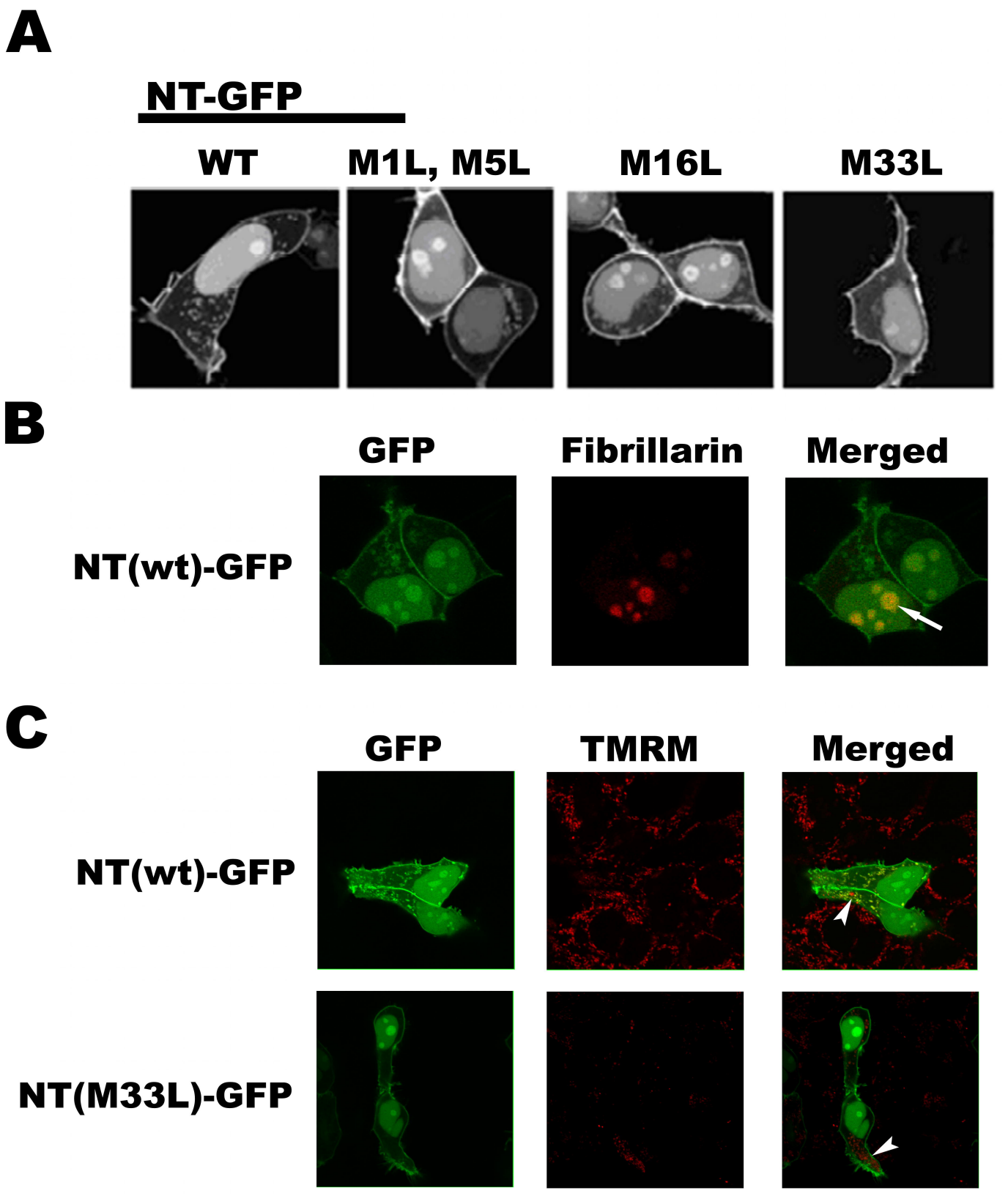
A
NT-GFP
WT
M1L, M5L
M16L
M33L
B
GFP
Fibrillarin
Merged
NT(wt)-GFP
C
GFP
TMRM
Merged
NT(wt)-GFP
NT(M33L)-GFP

Figure 5

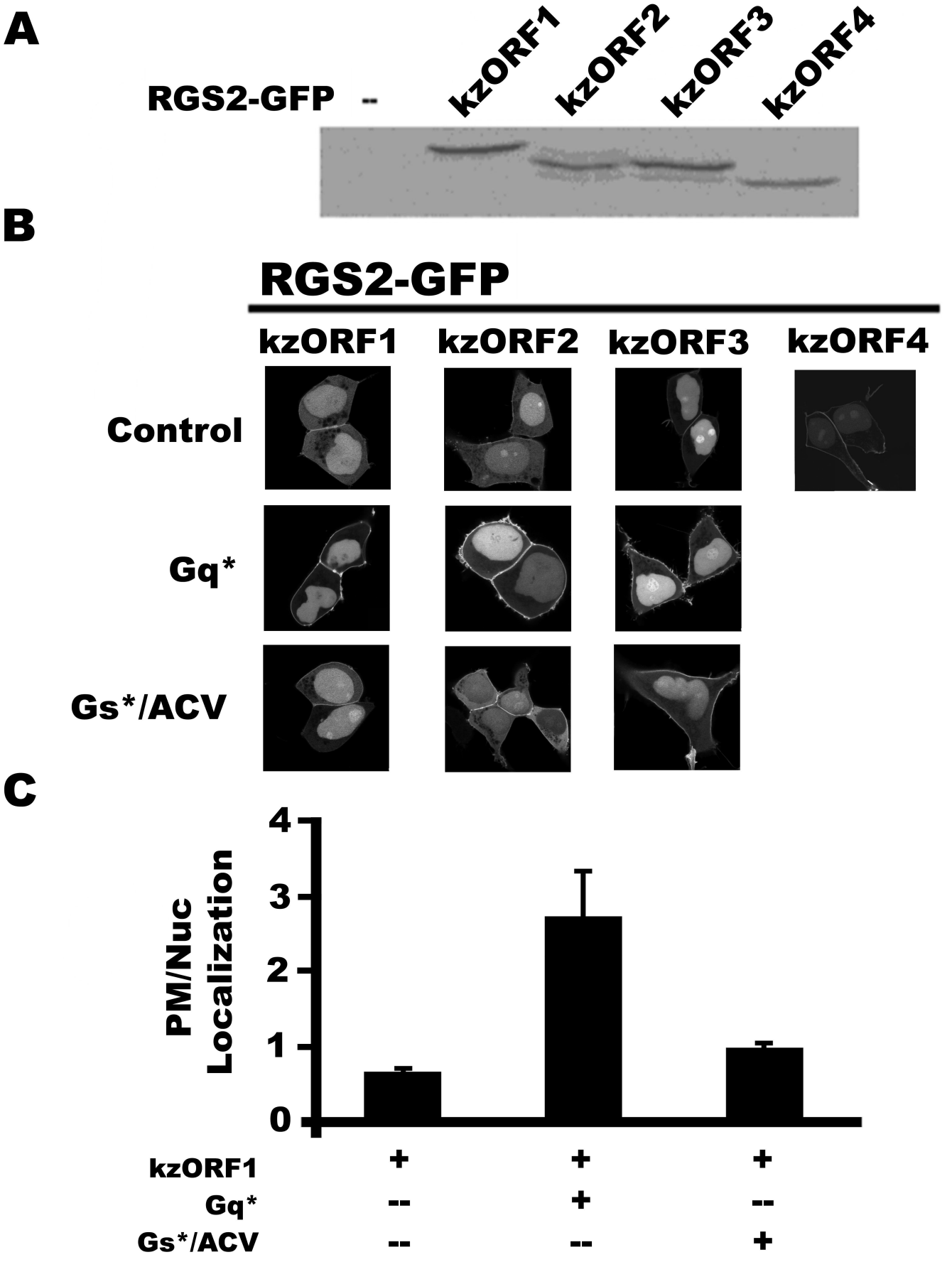
A
RGS2-GFP --
kzORF1
kzORF2
kzORF3
kzORF4
B
RGS2-GFP
kzORF1
kzORF2
kzORF3
kzORF4
Control
Gq*
Gs*/ACV
C
PM/Nuc Localization
0
1
2
3
4
kzORF1 + + +
Gq* -- + --
Gs*/ACV -- -- +

Figure 6

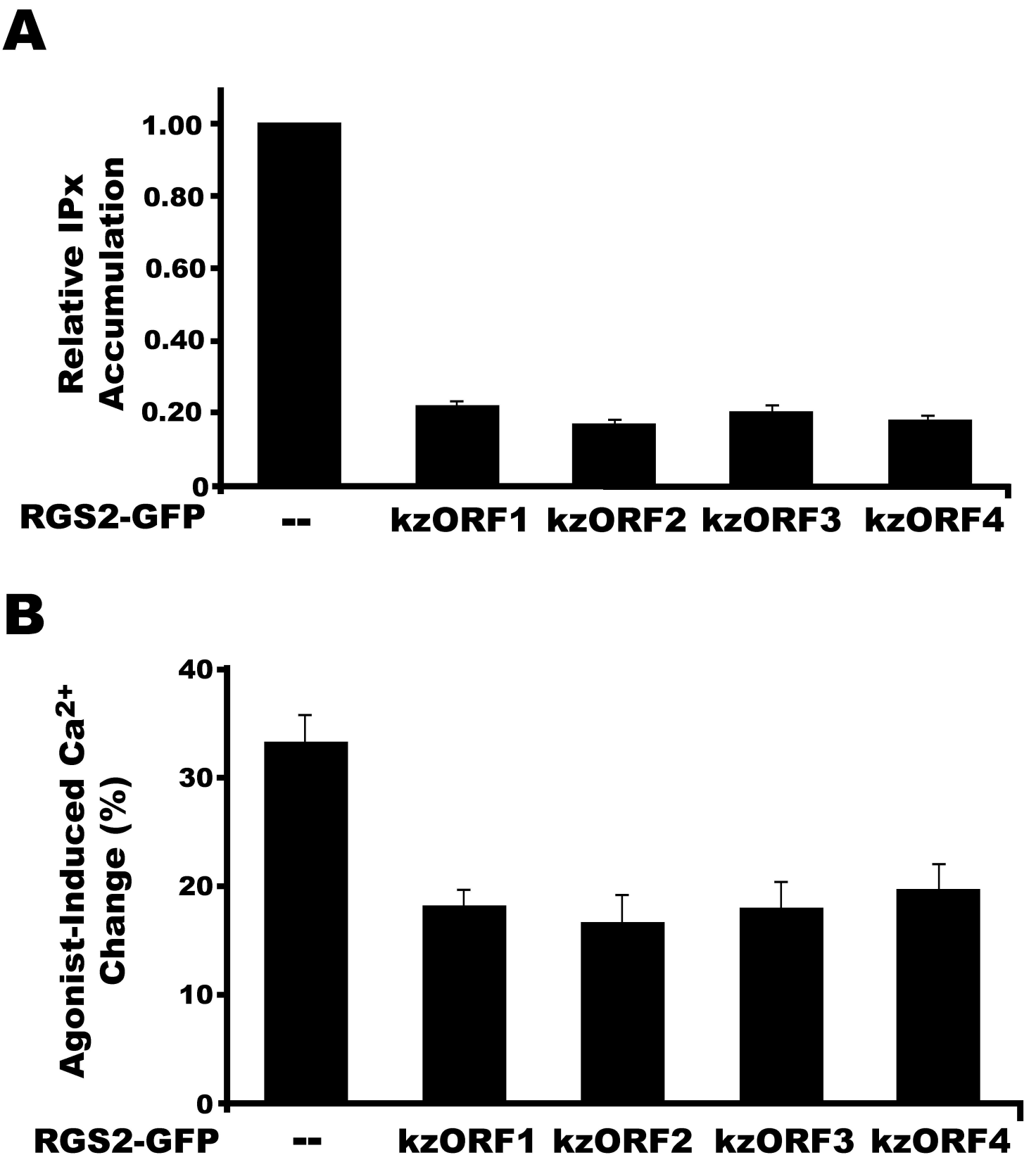
A
Relative IPx Accumulation
1.00
0.80
0.60
0.40
0.20
0
RGS2-GFP
--
kzORF1
kzORF2
kzORF3
kzORF4
B
Agonist-Induced Ca2+ Change (%)
40
30
20
10
0
RGS2-GFP
--
kzORF1
kzORF2
kzORF3
kzORF4

Figure 7

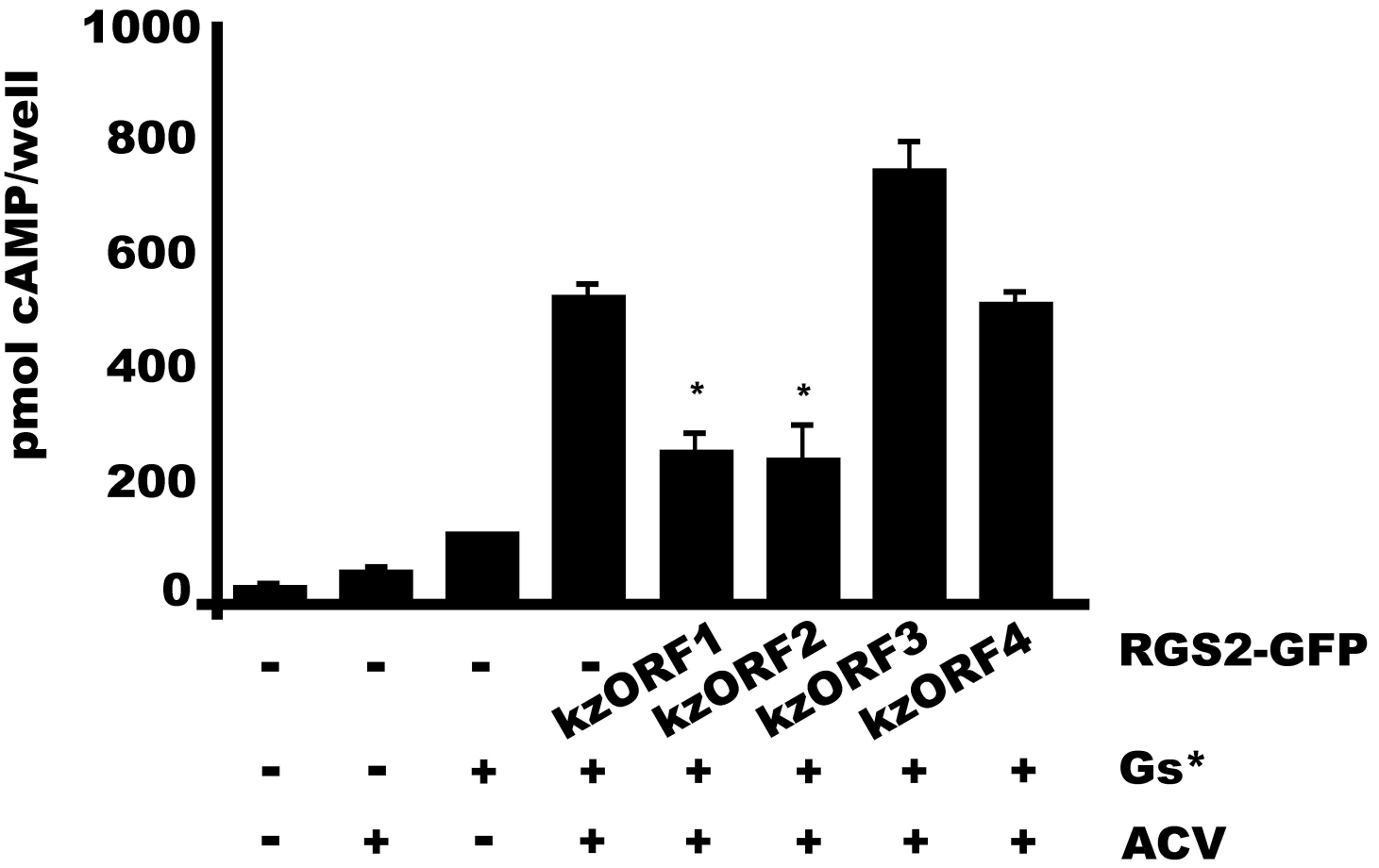
pmol cAMP/well
1000
800
600
400
200
0
*
*
kzORF1
kzORF2
kzORF3
kzORF4
RGS2-GFP
- - - - + + + +
Gs*
- - + + + + + +
ACV
- + - + + + + +

Figure 8

A

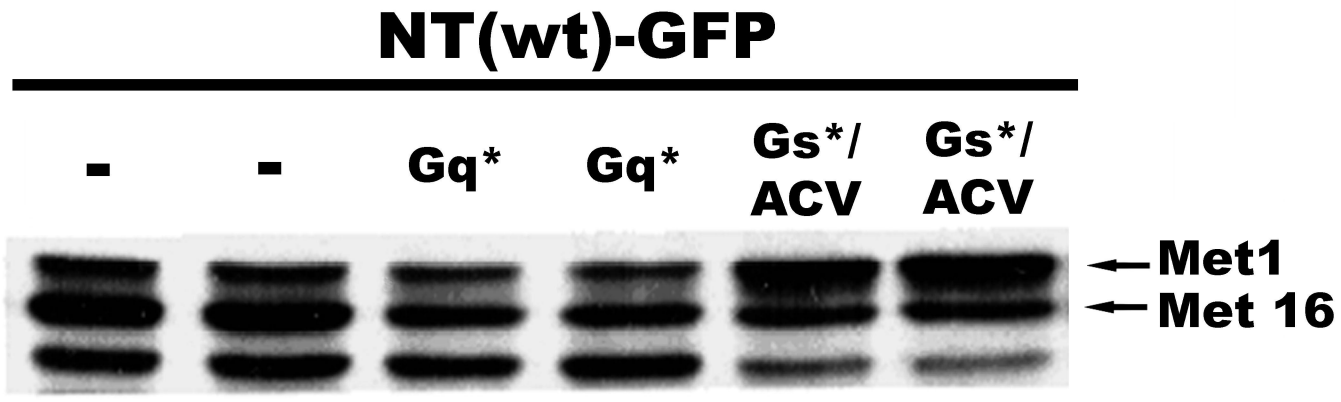
NT(wt)-GFP
-
-
Gq*
Gq*
Gs*/ ACV
Gs*/ ACV
Met1
Met 16

B

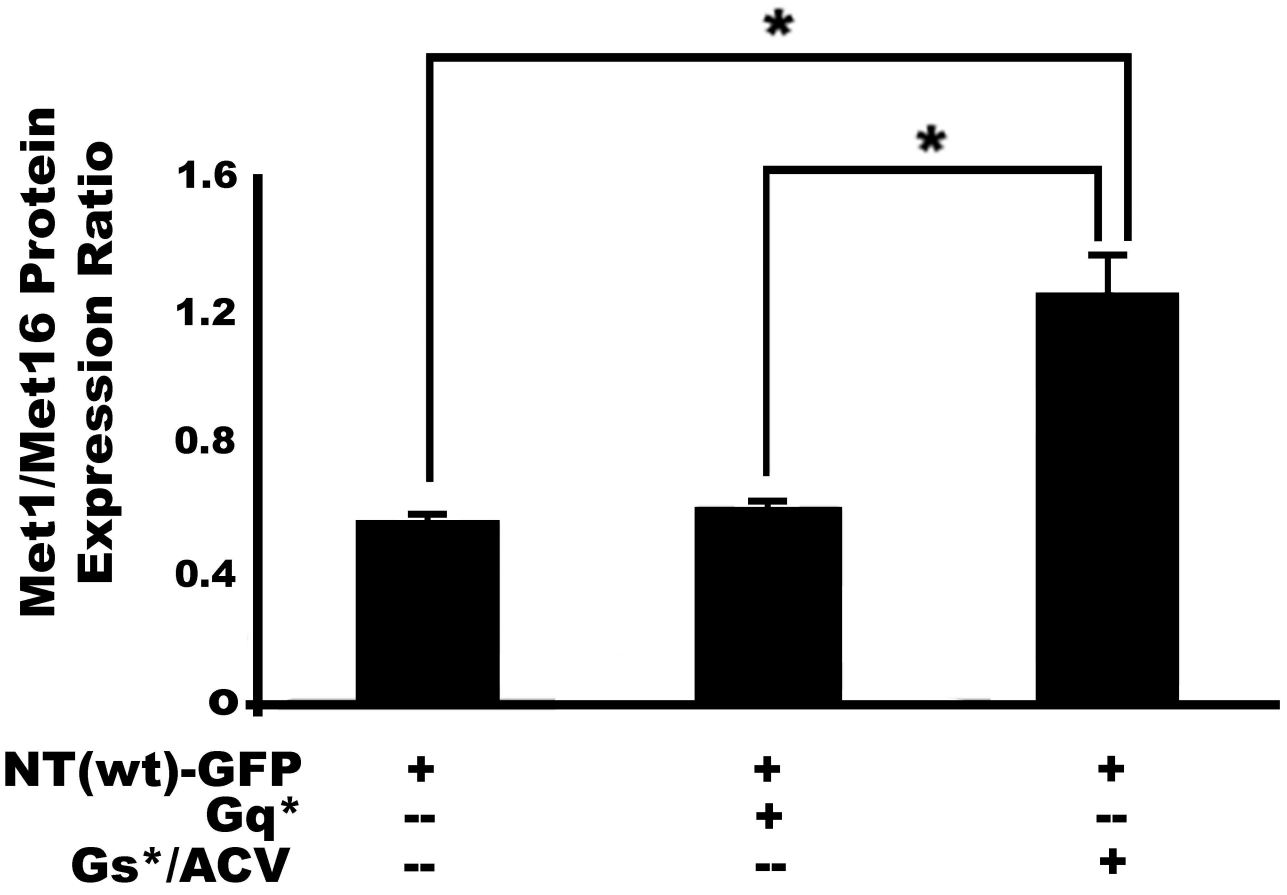
*
*
Met1/Met16 Protein Expression Ratio
1.6
1.2
0.8
0.4
0
NT(wt)-GFP + + +
Gq* -- + --
Gs*/ACV -- -- +